Ocean Modelling 190 (2024) 102401

Contents lists available at ScienceDirect

Ocean Modelling

journal homepage: www.elsevier.com/locate/ocemod

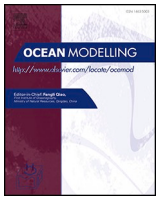

Debunking common myths in coastal circulation modeling☆

Y. Joseph Zhang [a,*], Joshua Anderson [b], Kyungmin Park [c], Chin H. Wu [b], Spenser Wipperfurth [d], Eric Anderson [e], Shachak Pe'eri [f], Dmitry Beletsky [g], Daniel Titze [h], Emanuele Di Lorenzo [i], Saeed Moghimi [j], Gregory Seroka [j], Edward Myers [j], Ayumi Fujisaki-Manome [g], John Kelley [j]

[a] Virginia Institute of Marine Science, William & Mary, Gloucester Point, VA, USA
[b] Department of Civil and Environmental Engineering, University of Wisconsin-Madison, Madison, WI, USA
[c] Pacific Northwest National Laboratory, Seattle, WA, USA
[d] Georgia Institute of Technology, Atlanta, GA, USA
[e] Department of Geophysics, Colorado School of Mine, CO, USA
[f] NOAA National Geodetic Survey, Silver Spring, MD, USA
[g] Cooperative Institute for Great Lakes Research (CIGLR), School for Environment and Sustainability, University of Michigan, Ann Arbor, MI, USA
[h] Great Lakes Environmental Research Laboratory, NOAA, Ann Arbor, MI, USA
[i] Earth, Environmental, & Planetary Sciences, Brown University, Providence, RI, USA
[j] Coast Survey Development Laboratory, NOAA, Silver Spring, MD 20910, USA

ARTICLE INFO

Keywords:
Cross-scale coastal modeling
DEM
Coastal modeling principles
SCHISM

ABSTRACT

Despite tremendous progress in algorithm development, computational efficiency and transition into operations over the past two decades, coastal modeling still lacks scientific rigor due to proliferation of many 'gray' areas related to various modeling choices made by modelers. In this paper, we propose some guiding principles for the modeling community to improve performance, and we also debunk commonly held myths that make the coastal modeling lack rigor. Using our own experience in developing seamless cross-scale unstructured-grid based models for the past two decades, we describe in unprecedented detail the end-to-end modeling process (i.e., from digital elevation models (DEMs) to mesh generation to post analysis), and demonstrate that defensible modeling is within reach for any end user by following three guiding principles: (1) Bathymetry is a first order forcing in coastal domains and thus should be respected in all aspects of modeling; (2) Oceanographic processes are driven across multiple spatial scales and so models should enable appropriate resolution as needed; and (3) Model assessment should focus on physical processes. Through qualitative and quantitative model assessments, we demonstrate the fundamental role played by bathymetry/topography as embedded in DEMs in making the results defensible, which is unfortunately glossed over in many modeling studies. Focusing on process-based assessment simplifies the calibration process. A major conclusion of this work is that model developers and operators should maximize the scientific rigor for *in silico* oceanography by avoiding some common pitfalls that rely on error compensation at the expense of representation of physical system processes. We present some best practice procedures for defensive and trustworthy numerical modeling.

1. Introduction

Coastal oceanography grapples with many challenging nonlinear processes at a myriad of scales (from minutes to centuries and from meters to 100 s of kilometers) that are directly linked to the complex shoreline geometry, nearshore bathymetry and strong forcing functions. Over the past two decades, the coastal modeling community and the available products have grown exponentially thanks to the convergence of advancements made in observation techniques, high-performance computing technology, and improvement in numerical algorithms (see reviews by Klingbeil et al., 2018; Fringer et al., 2019). As a result, real-world simulations have become widely available in forecast, engineering analysis and climate predictions (Wilkin et al., 2017).

Despite the tremendous progress mentioned above, current coastal ocean modeling efforts still suffer from many shortcomings and lack of scientific rigor due to proliferation of many 'gray' areas. Those gray

☆ Submitted to: Ocean Modelling Special Issue "In silico oceanography via seamless cross-scale modeling: Are we there yet?"

* Corresponding author.
E-mail address: yjzhang@vims.edu (Y.J. Zhang).

https://doi.org/10.1016/j.ocemod.2024.102401
Received 23 March 2024; Received in revised form 6 June 2024; Accepted 21 June 2024
Available online 26 June 2024

areas are related to many seemingly arbitrary and subjective decisions made by modelers and have historically hampered the greater adoption of unstructured-grid (UG) models but equally plagued structured-grid (SG) models. Some common gray areas ('myths') will be introduced, demonstrated, and discussed from concrete examples and application cases using different models in this paper. We should mention that this problem of the common gray areas is not confined only to *in silico* oceanography. Related fields of hydrography and cartography have also struggled with this issue (Skopeliti et al., 2020). Following an international effort, observation and bottom measurements are defined using Total Propagated Uncertainty (TPU) (International Hydrographic Organization, or IHO 2020). With the advancements in sensor technology and geodetic control, it is possible to accurately evaluate the uncertainty from all components used in data collection. For example, the associated vertical component of the TPU (2 sigma or standard deviation) for bathymetry DEMs (digital elevation models) using ocean mapping technologies can range between 10 cm to 1 m, depending on the technology (i.e., Sonar, Lidar, or Satellite Derived Bathymetry) and water depth (Pe'eri et al., 2014).

The benefit from the advancement in sensor technology is however greatly negated by error compensation in numerical models; the latter is a more prevalent problem than many researchers realize and ignoring it may affect the model's ability to faithfully simulate processes. We will expound this and other critical issues in this paper, with a particular focus on the representation of bathy-topo DEM in circulation models. By definition, *in silico* oceanography seeks to realistically simulate processes. An overarching goal for *in silico* oceanography should therefore be to maximize scientific rigor by minimizing pitfalls that rely on error compensation at the expense of representation of physical system processes. We therefore define three guiding principles for *in silico* oceanography:

1. **Bathymetry is a first order forcing in coastal domains**. Hence, observation-based DEM data should not be smoothed or otherwise manipulated beyond the native resolution of the numerical grid (in much the same way the observed surface elevations should not be altered).
2. **Oceanographic processes are driven across multiple spatial scales**. Hence, grids must be as high spatial resolution and extend over as large geographic domain as required by the processes and known forcing (within available computational limits), including some ultra localized processes.
3. **Assessment should focus on processes**. Hence, traditional quantitative error metrics, while useful, are not a substitute for feature-based metrics and should not distract or mislead high-fidelity representation of processes.

In this paper we will describe an end-to-end coastal modeling procedure from beginning (preparation of DEM for mesh generation) to end (analysis of results) using a state-of-the-art community UG model (SCHISM; schism.wiki, last accessed in March 2024), in light of the three principles. When appropriate, we will contrast SCHISM's approach against some common practices adopted by other models. The goal of this paper is to raise community's awareness of the fundamental role the DEM plays in *in silico* oceanography and thus encourage full disclosure of this critical piece of information in their study descriptions. On the other hand, artificially manipulating DEM in computational (structured or unstructured) grids to fit the model needs would significantly confound the error sources and make the results indefensible (Ye et al., 2018; Cai et al., 2020). We remark that while the importance of DEM has been widely acknowledged in the modeling community, in practice it is often forgotten and rarely enforced or verified in the modeling procedure.

We note that SG coastal models (see Klingbeil et al. (2018) for a review) do not have the flexibility for local refinement (which is essential for coastal modeling) and have to rely on nesting to locally resolve features within reasonable computational costs, which is cumbersome at best and hinders the interpretation of interaction of scales that are inherent in coastal systems. For example, the most salient features for the estuarine models to capture are river and navigation channels, where three-dimensional (3D) processes and gradients are most pronounced. However, even with nesting or curvilinear coordinates, SG model grids' representation of channels is often inadequate (Hood et al., 2021). Therefore, we will mostly focus our discussions on UG models in this paper, but it should be kept in mind that the importance of DEM applies to all types of models.

Two study sites in the U.S. will be used in this paper as examples to demonstrate the principles: 1) Lake Champlain, a freshwater lake, and 2) New York Harbor (NYH), which represents a typical estuary system. The second study site (NYH) is also part of NOAA's Unified Forecast System (UFS) Coastal Applications Team model evaluation that is working to develop model evaluation recommendations for selecting NOAA's next-generation numerical oceanographic circulation prediction models for coastal applications, such as safety of navigation, risk reduction and total water levels. The paper thus sheds important clues on how different models ingest DEMs and physical forcings. An important outcome of both this work and NOAA's UFS project is to foster an open conversation on rigorous and defensible modeling that minimizes gray areas, with special attention paid to model representation of realistic bathy-topo digital elevation models (DEMs), which are also used in their native format for mapping and charting.

In Section 2, we describe the DEMs and other types of observation datasets used in this paper. Section 3 details the model setup process, with focus on the UG mesh generation. In Section 4, we demonstrate an evidence based, iterative model calibration approach to progressively improve the model, with a focus on the model's representation of key processes and with guidance from DEMs throughout the whole process. With process-based assessment, we primarily ask the question whether or not a model is able to capture important processes of interest (e.g., stratification, salt intrusion, upwelling, etc.) with sufficient skill. The process-based assessment often requires minimal model 'tuning' if the model is robust and physically and numerically sound. A short summary is given in Section 5.

Table 1
Uncertainty coefficients used to calculate the maximum allowable *TVU*, defined as $TVU = \sqrt{a^2 + (bd)^2}$, for different ocean mapping applications (IHO 2020). Special Order is the high-quality surveys with full bottom coverage (100 %) with an ability to identify features as small as 1 m^3. Order 1 is the standard quality, with full coverage (100 %) but the quality can vary. If it is possible to detect features as small as 2 m^3, then this is Order 1a. If not, then this survey is Order 1b. Order 2 includes all low-quality surveys, is the least stringent order, and is intended for areas where the depth of water is such that a general depiction of the bottom is considered adequate. This order requires a minimum of 5 % areal coverage and is recommended for use in water depths deeper than 200 m.

IHO order	*a (m)*	*b (-)*	TVU_{max} (m)
Special Order	0.25	0.0075	0.34
Order 1	0.5	0.013	0.63
Order 2	1.0	0.023	1.21

2. Observation

2.1. DEMs

Since the 1990s ocean mapping surveying has advanced in the survey technologies being used (i.e., from lead line and single-beam SONAR systems to multi-beam echosounder and airborne Lidar technologies), through geodetic technologies (from LORAN—C to Global Navigation Satellite Systems), to synchronization techniques and calibration methodologies. As a result, it is possible to achieve seamless coverage from ocean to land at sub-meter resolution, both horizontally and vertically. The International Hydrographic Organization (IHO)

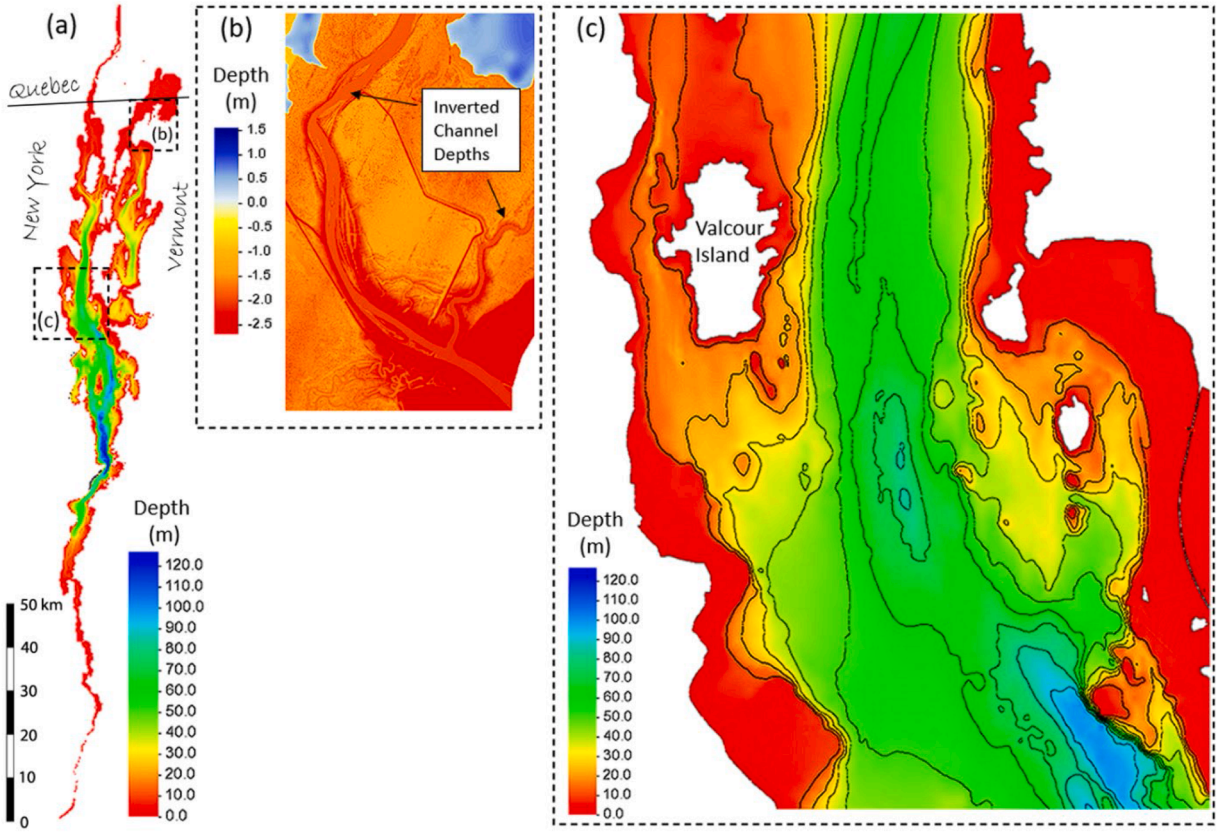

Fig. 1. DEM for Champlain. Positive/negative depths indicate water/land, respectively. (a) Entire domain; (b) Zoom-in to show inverted river channel in shallow area of DEM (i.e. with thalweg elevation higher than surrounding); (c) DEM zoom-in near Valcour Island.

identified key components to the Total Propagated Uncertainty (TPU). They mentioned that "the ability of the survey system should be demonstrated by a priori uncertainty calculations", where the uncertainty calculations are predictive and must be calculated for the survey system "as a whole, including all instrument, measurement, and environmental uncertainty sources" (IHO 2020). As a result, there is an international consensus that the vertical component of uncertainty (total vertical uncertainty, TVU) is depth dependent, and the maximum

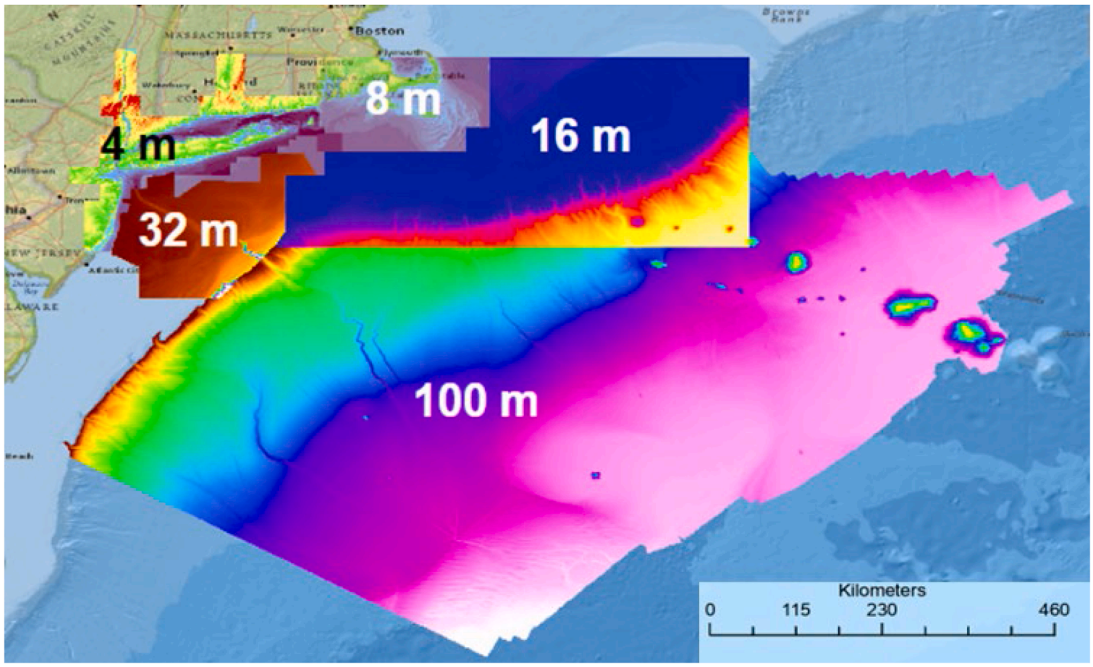

Fig. 2. DEMs used for NYH, with horizontal resolution for each section overlaid. Also see Table 2. No smoothing is done across DEM tiles on the computational mesh, which might lead to some minor artifacts. Detailed comparison of how different models 'see' the DEMs will be shown in other figures.

Table 2
DEM sources for NYH case. NBS = National Bathymetric Source; NCEI = National Centers for Environmental Information; CCOM: Univ. of New Hampshire's Center for Coastal and Ocean Mapping.

Resolution	4 m	8 m	16 m	32 m	100 m
Source	NBS	NBS	NCEI	NCEI	CCOM
Survey data date	2000–2024, with shallow band data from the 1930′s	2000–2024, with shallow band data from the 1930′s	1970′s	1970′s	2004 to 2012

allowable TVU (2 sigma) for ocean mapping is defined using simplified root mean square of $a^2 + (b \times d)$, where d is the depth and the coefficients a and b represent the portions of the uncertainty that are independent of and dependent on the depth, respectively (Table 1).

For modeling purposes, high-quality DEM products that are vertically referenced to a regional or global datum, contain a vertical uncertainty (2 sigma) that can range from 10 cm to 1 m. These high quality DEMs are common within the US territories and in many locations around the world that use modern survey technologies. DEM errors belong to the category of epistemic (instead of aleatoric) uncertainty, and thus can and have been reduced with better observation techniques over time. We emphasize here the word 'high-quality' instead of commonly used 'high-resolution', as the latter describes sampling rates or interpolation of a DEM product and may not be a good measure for the quality of the survey data (Huang et al., 2022). Due to varied priority and resource limitations, the DEM quality inevitably varies, which should be taken into account in modeling. In general, the model should utilize DEMs of the best quality as much as possible. Once the DEMs have been selected, however, we should treat them as ground truth just like other types of observations (e.g. surface elevation) with an associated uncertainty, until better field evidence emerges. This operational guideline is in accordance with the first guiding principle for *in silico* oceanography mentioned in Section 1. We differentiate DEM uncertainties (TVU) from the artificial manipulations done by some model applications; we will illustrate with both study sites that the artificial manipulations are often orders of magnitude larger than TVU.

Lake Champlain is a bi-national lake bordered by New York on the west side, Vermont on the east side, and Quebec in the north (Fig. 1). In recent years, severe floods caused by intense rain events and spring runoff caused significant destruction of property and infrastructure in the Lake Champlain Basin. In addition, high lake water levels provided conditions for more shoreline destruction by wind waves and storm surges that build over the long north-south fetch of the lake (Beletsky et al., 2022; Titze et al., 2023; Anderson et al., 2024). The DEMs for Lake Champlain are derived from Environment and Climate Change Canada (ECCC 2015). However, close inspection reveals some issues with shallows; Fig. 1b shows an example where the river channel has a lower depth (higher elevation) compared to the surrounding area. Therefore, we decided to retain the highly questionable bathymetry information from another UG model ('Model A' hereafter) in the shallows, which at least allows the delivery of river flow into the lake, until better DEMs are found. The original DEM is only used for the deeper basins. This case was selected to illustrate that even in systems with poor quality DEMs it is still possible to make qualitative assessment for models (Section 4).

NYH is typical of meso-tidal estuaries in the US East Coast, with significant economic and ecological values (Park et al. 2024). For NYH, we used a mixture of DEM sources that cover the shelf and estuary and rivers with 4 m to 100 m resolutions (Fig. 2; Table 2). Fortuitously, during the UFS project we were able to get direct help from the DEM provider, NOAA's Office of Coast Survey (OCS) after some DEM issues were identified. Therefore, this case provides a perfect testbed of a natural laboratory to illustrate the model's sensitivity to DEM quality, as we will show in the next two sections.

2.2. Other types of observation

The model skill is assessed against available observation stations for the two systems. For Lake Champlain, the main observations are water level observations at 6 gauges around the lake. In addition, temperature profiles mostly in the deeper part of the lake were also used for skill assessment. In this paper, we will only show validation against temperature profiles, whereas additional assessments are available in Anderson et al. (2024).

For NYH, observations of water surface elevation, water velocity, salinity and water temperature are available at multiple stations for the selected testbed period (2021–2022), thus allowing a more comprehensive skill assessment. All observation data shown in this paper and Park et al. (2024) have been quality controlled and are generally referenced to the vertical datum of NAVD88.

3. Model setup

We use the open-source community model SCHISM in this paper to illustrate a rigorous end-to-end modeling process. SCHISM solves the hydrostatic, Boussinesq, primitive equations on a hybrid triangular-quadrangular unstructured grid in the horizontal and hybrid Localized Sigma Coordinates with Shaved Cells (LSC^2) grid in the vertical (Zhang et al., 2015, 2016). SCHISM is the successor to two community models we developed: ELCIRC (Zhang et al., 2004) and SELFE (Zhang and Baptista, 2008); all three models shared a common theme of realistically representing DEM and processes. SCHISM is grounded on an accurate, robust and efficient semi-implicit time stepping scheme (with no mode splitting) and a hybridized finite-element and finite-volume formulation. The numerical dissipation is kept low with a judicious combination of higher-order, monotone schemes (Ye et al., 2019). Significantly for our purpose of rigorous model assessment, the model's ability to use original unsmoothed DEMs and very high local resolution as required by processes is crucial to satisfy the first and second principles. The solid representation of realistic physics using advanced, robust numerical schemes inside SCHISM greatly minimizes the need for error compensation and makes important forcing functions transparent to interpret; for example, improvement in the DEM quality would immediately translate into skill improvement (cf. Section 4.1.2). For comparison purpose, we will contrast SCHISM with another coastal model (Model A) that uses bathymetry smoothing and other types of artificial manipulation for model performance, which is common practice among many coastal models. Freeing models from the need for artificial manipulation is a positive major step toward defensible coastal modeling.

The first and a key step for UG model setup is the mesh generation. Traditionally mesh generation has long been considered as an 'art' rife with seemingly arbitrary decisions. We debunk this myth by detailing SCHISM's mesh generation process that has a primary goal: to realistically capture key DEM features that are deemed important for the processes under study. Consistent with the first and second principles, the primary goal of mesh generation for SCHISM is to capture all important features in the DEMs, regardless of their sizes, that may influence the model's ability to faithfully represent the targeted processes. In this sense, mesh generation for SCHISM is "straightforward" as the mesh should be designed to capture realistic physics (including bathymetry as well as physical forcings) instead of accommodating the numerics. In other words, many artificial manipulations to e.g. stabilize the model are unnecessary in SCHISM. Consequently, it is quite possible to automate the process with scripts; a recent example of a DEM-driven mesh generation tool is presented in Ye et al. (2023). We remark that bathymetry smoothing, either during or after the mesh generation process, has been demonstrated to introduce systemic changes that detrimentally impact the model skill and result in error compensation that is difficult to untangle (Ye et al., 2018 for physical processes; Cai et al., 2020 for biochemical processes).

In this section, we will only describe the first iteration of the mesh

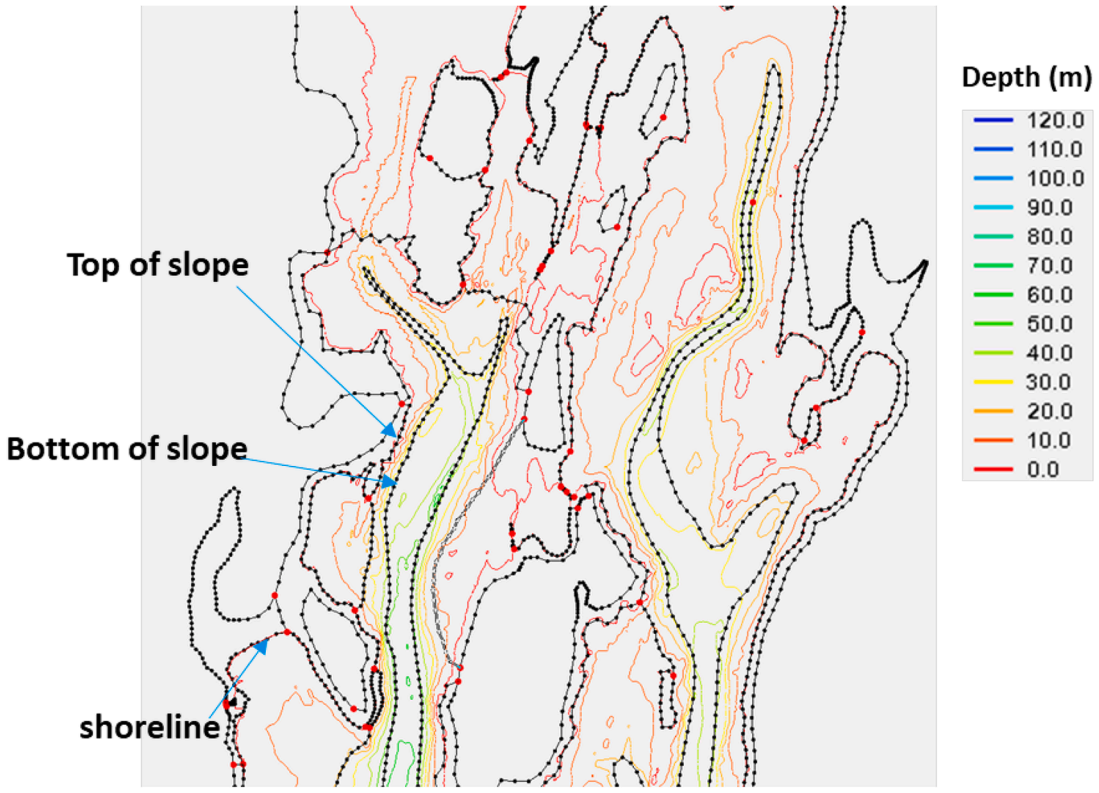

Fig. 3. SMS map for Lake Champlain. Positive depths denote water (below datum). The red and black points are "nodes" and "vertices", respectively, in SMS terminology; each arc is bounded by 2 "nodes" and has multiple interior "vertices".

generation process (before any model adjustment) using a mesh generation tool, SMS (aquaveo.com), followed by other model setup details. We will continue this discussion in Section 4 by demonstrating the importance of remeshing whenever DEM is improved, or calibration needs arise. The principle illustrated here applies to other mesh generation tools as well.

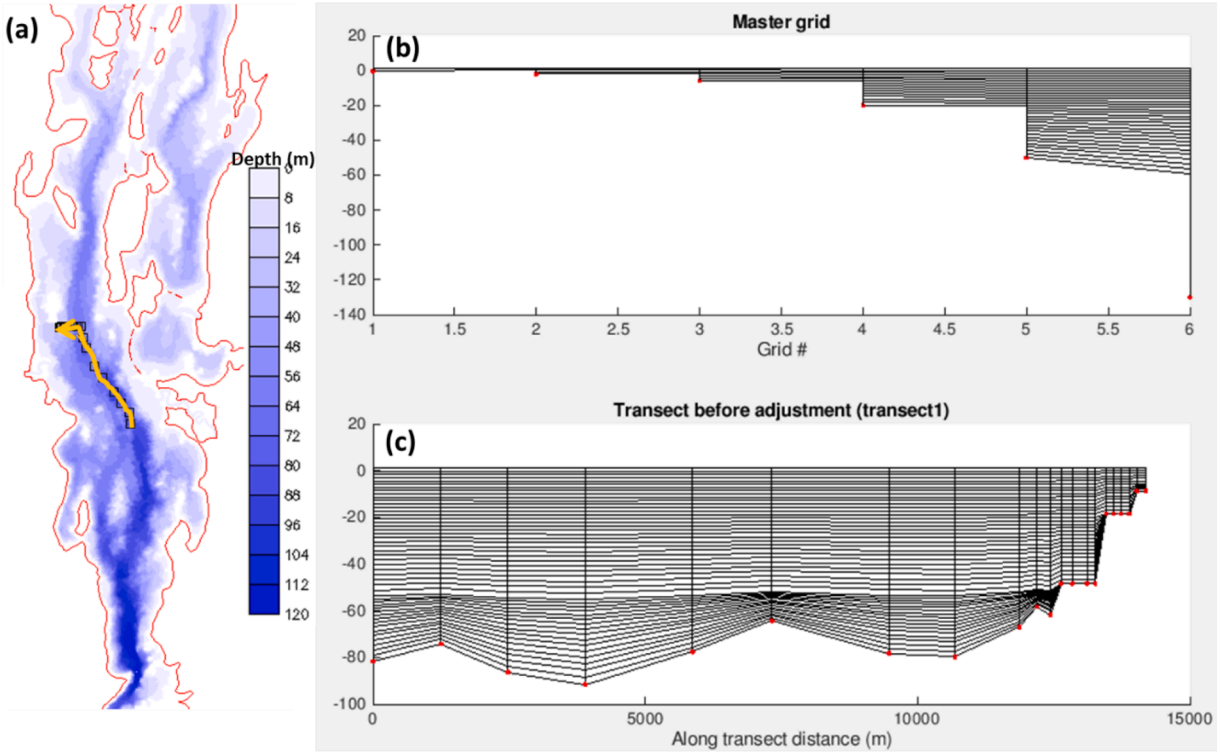

Fig. 4. Vertical grid used for Lake Champlain. (a) Transect location, first along the channel and then into the shoal (the color indicates depths); (b) Master grid used in LSC^2; (c) Final vertical grid along the transect.

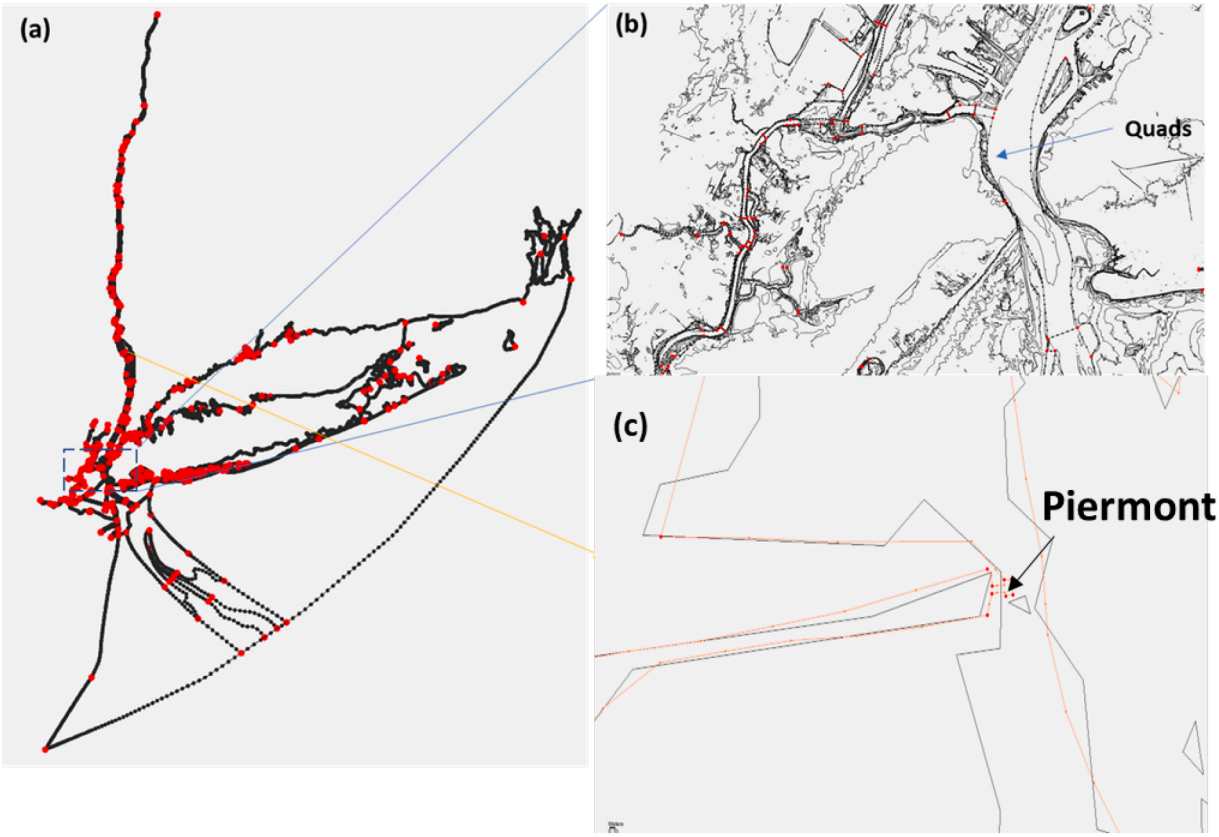

Fig. 5. SMS map for NYH. The faint black lines in (b) are isobaths of −10, −1,0,1,2,3,4,5,6,8,10,20,30,40 and 50 m (with positive numbers denoting water). The black lines in (c) are isobaths of 0, 2 and 5 m, respectively. The location of the gauge (Piermont) is accurately represented in the SMS map using multiple arcs (red lines) to delineate the jetty and pier.

3.1. Lake Champlain

3.1.1. Mesh generation

Most mesh generating tools adopt a similar strategy to construct an UG mesh, by sub-dividing the whole domain into smaller non-overlapping polygons (cf. Fig. 3). The mesh resolution is usually specified via the vertices of arcs that bound each polygon, although other methods such as density paving (i.e. with cell size function defined on a separate grid) exist. The tools then create the entire mesh by meshing each polygon first and making sure the vertices match across polygonal boundaries (with necessary adjustment if needed). This 'divide-and-conquer' approach has the advantage of being able to easily scale up to very large meshes (Ye et al., 2023).

The lake is first "digitized" with a number of representative 'arcs' that form polygons for each sub region (Fig. 3). The selection of arcs depends on specific processes to be captured. In most nearshore systems, the important DEM features include steep slopes (e.g., channel edge) and structures that guide the flow (e.g., jetties, breakwaters, etc.). The bathymetric slope in this lake is relatively steep. Therefore, SMS arcs generally follow those steep slopes (Fig. 3); special treatment near Thompson's Point, which is the steepest location in the lake (cf. Fig. 17), will be described in Sections 4.1.1 and 4.4.1. Typically, we use one arc each to delineate the top and bottom of slopes, identified by convergence of bathymetric contours (Fig. 3). The shoreline is also delineated by arcs in this case. In general, it's sufficient for those arcs to reasonably follow the contours and they do not need to be extremely precise (because the mesh resolution is generally coarser than the DEM's); also, the precise capturing of the shoreline is not necessary as the latter is moving over time. Whether or not to use arcs to represent other interior features is dependent on the need for specific processes (e.g., higher resolution may be requested near a coast to better capture coastal upwelling). Occasionally, additional arcs & polygons are created to simplify connectivity and prevent SMS from crashing (not applicable in this paper). The default SMS meshing algorithm ('paving' with pure triangles) can easily resolve features in wide and open water bodies but faces challenges for elongated features like channels. The latter can be effectively meshed using quads (cf. Section 3.2.1).

3.1.2. Other inputs

SCHISM's highly flexible and robust LSC^2 vertical gridding system (Zhang et al., 2015) is used, with 1–48 layers covering different depths (Fig. 4). Note that the surface is well resolved throughout, and the bottom is less resolved than the surface. It's easy to resolve both by re-designing the 'master' grid (Zhang et al., 2015) but this is not carried out here. The z-coordinate planes are close to horizontal in most of the interior of the column (Fig. 4), thus alleviating pressure-gradient errors.

For simplicity, a constant bottom roughness of 0.1 mm is used, which gives adequate model skill. The atmospheric forcing is derived from the NOAA High-Resolution Rapid Refresh (HRRR; Benjamin et al., 2016). Constant albedo and water type (for attenuation of short-wave radiation) are used, together with a turbulence closure scheme of *k-kl* (Umlauf and Burchard 2003). The simulation starts on April 1, 2017, and lasts 270 days. The time step used in this case is 90 s, and the 2nd-order transport solver (TVD^2) is used for the tracer transport. All inputs for the final setup (after the calibration was done as shown in Section 4) can be found in the file LC_05b_in.tgz of Supplementary Materials.

3.2. New York harbor

3.2.1. Mesh generation

Channels play a pivotal role for many estuarine processes such as gravitational circulation, salt intrusion, lateral circulation, and

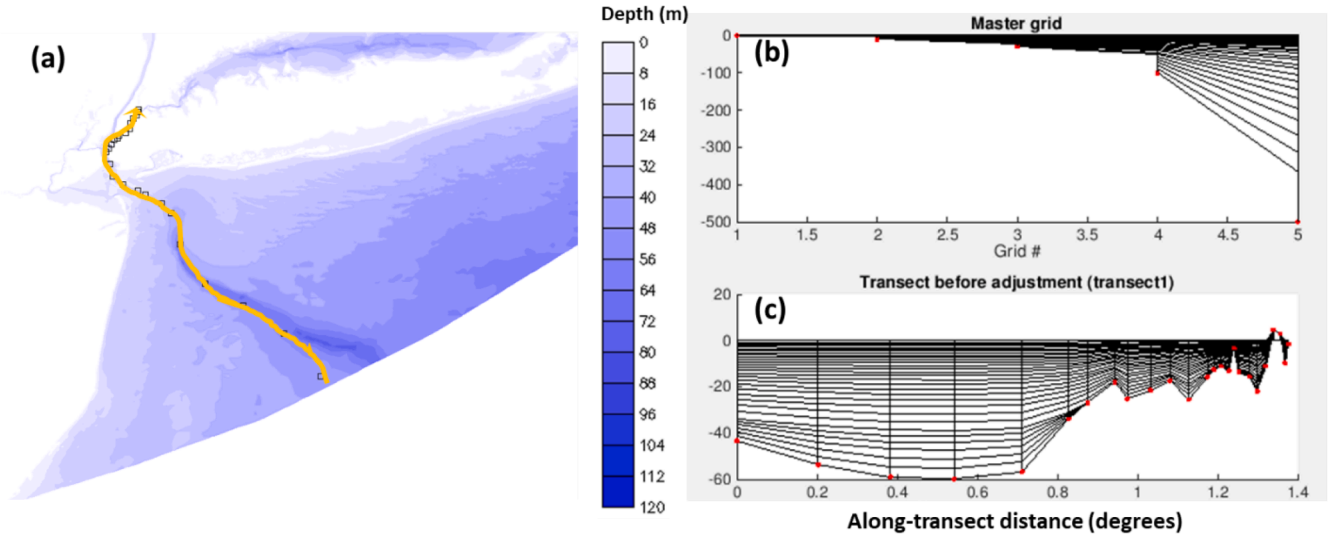

Fig. 6. Vertical grid used for NYH. (a) Transect location (from Hudson Canyon into Hudson River and East River); (b) Master grid; (c) Vertical grid along the transect.

differential advection, etc. High-gradient zones are usually found in and around the channels. Therefore, an important task for mesh generation is to accurately resolve the channels. We remark here that unfortunately few models (UG or SG) pay adequate attention to resolving channels due to various limitations (whereas interestingly, often fine resolution is used near the shoreline, where the 3D processes are less pronounced). Following the same guideline as described in the lake case, we identify and delineate the top and bottom of channels in most rivers (Fig. 5). We use quadrilaterals to represent channels as much as possible ("patches" in SMS) to achieve three goals: (1) flow-aligned quads are known to be more accurate (Holleman et al., 2013); (2) unlike triangles, quads can easily and very precisely control the along- and especially cross-channel resolution, which is important for 3D processes like tracer transport; (3) they significantly reduce the mesh size when there are many channels (for large meshes the savings can be on the order of 10 times). On the other hand, quads are well known to be inflexible in following complex geometry, and for that, triangles can be added as needed to provide flexibility (as SMS does).

Model skill assessment is often conducted at gauges that are located in sheltered shallow locations, for maintenance and other purposes. To faithfully capture the local details that may exert impact on the model results (Huang et al., 2022), careful examination of DEMs and the SMS map is done at all gauges to avoid a common problem related to wetting and drying. An example is shown in Fig. 5c for the Piermont station in the upper Hudson River, where we have used multiple arcs to delineate the water body and dry land around the station. Another example will be shown in Section 4.3 (cf. Fig. 16). Note that the wetting and drying issue originates from the linear interpolation method used in SCHISM and is often obscured by other artificial treatments used in other models (e.g., nearest wet node interpolation, bathymetry smoothing and other ad hoc manipulation). Another challenge for comparison at stations is the survey errors for the station location (which may also change due to ground subsidence, etc.). If the errors are sufficiently large that the station is found at dry spots, no mesh generation method can rectify the errors and, in this case, it is justifiable to nudge the station to a nearest wet spot. We remark that these types of stations are increasingly rare as the surveying techniques have improved in recent years.

3.2.2. *Other inputs*

A different LSC^2 vertical gridding system is used from the lake case, with 1–32 layers in the vertical dimension (Fig. 6). Besides the difference in the maximum depths in the two systems, more resolution is used here at 30 m reference depth to better capture the salt intrusion process.

The atmospheric forcing is also derived from HRRR. Constant albedo and water type (for attenuation of short-wave radiation) are used, together with a turbulence closure scheme of *k-kl*. The simulation starts on June 1, 2021, and lasts 120 days. The time step used in this case is 150 s, and the 2nd-order transport solver of TVD^2 is used to solve the tracer transport. Spatially variable viscosity and bottom friction are used for this case in order to maximize the quantitative skill, but spatially uniform inputs for these parameters can also produce quite good results (Park et al. 2024). All inputs for the final setup (after the calibration as shown in Section 4 was done) can be found in the file NYH_200a_in.tgz in the Supplementary Materials.

4. Model calibration and assessment

We discuss in this section several important topics related to the three principles, that are commonly encountered during the model calibration and assessment process. We start the discussion in Section 4.1 on the intimately related mesh and DEM issues to highlight the importance of faithfully conforming mesh to DEM without artificial manipulation and to describe the consequence otherwise (i.e., the first principle), particularly as far as the process-based assessment is concerned (the third principle). We demonstrate that by following these principles, SCHISM is very responsive to the improvement in DEM, as models should be (Section 4.1.2). In Section 4.2 we present the need for using linear interpolation from DEM instead of the nearest-point interpolation as the latter can introduce systematic biases that may be missed in point-wise comparisons (the third principle). In Section 4.3 we show a typical workflow from post-processing analysis to remeshing in order to improve the model; the local mesh refinement/adjustment is done to capture localized processes more accurately (the second principle). The evidence-based calibration is further elucidated in Section 4.4 using a few examples drawn from the two study cases to improve model skill; the goal is to make the calibration process as defensible as possible. The fact that bathymetry as represented by the DEM is one of the most fundamental forcings in the coastal regime and different models 'see' different bathymetry serves as a cautionary tale when users try to intercompare the numerical dissipation (Section 4.5). Finally in Section 4.6, we summarize the third principle by comparing process-based with traditional quantitative skill assessment. Focusing on the process-based assessment often simplifies the calibration process, avoids the gray area of error compensation, and thus maximizes model credibility. For this reason, we will mostly focus on process-based assessment here.

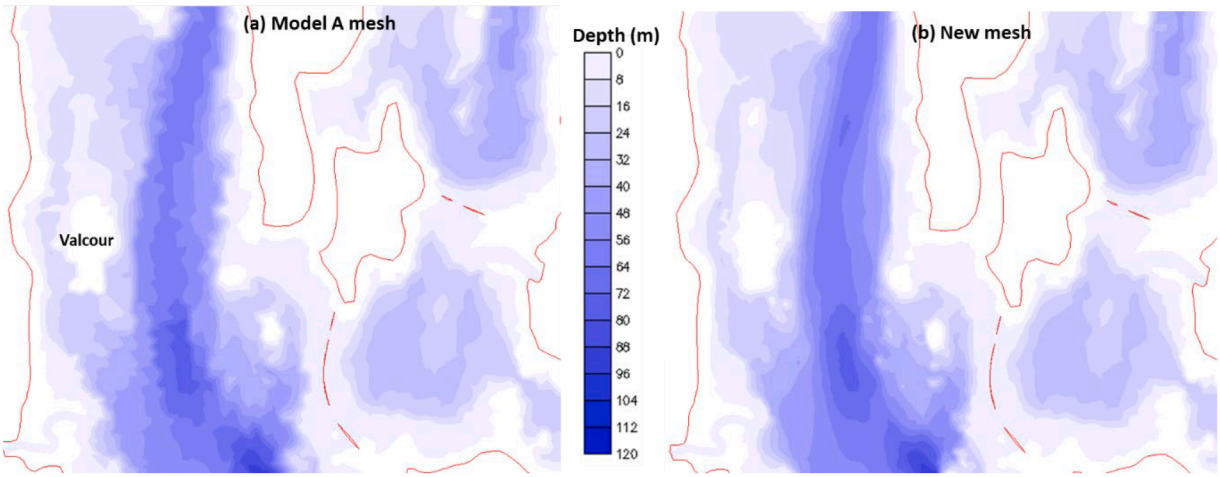

Fig. 7. Comparison of bathymetry as seen by (a) Model A mesh (with smoothing/manipulation) showing artificial jagged patterns in the channel near Valcour Island in addition to gentler slopes. (b) revised SCHISM mesh based on DEM. The DEM in this area is shown in Fig. 1. The resolution used in this area is similar between the two meshes.

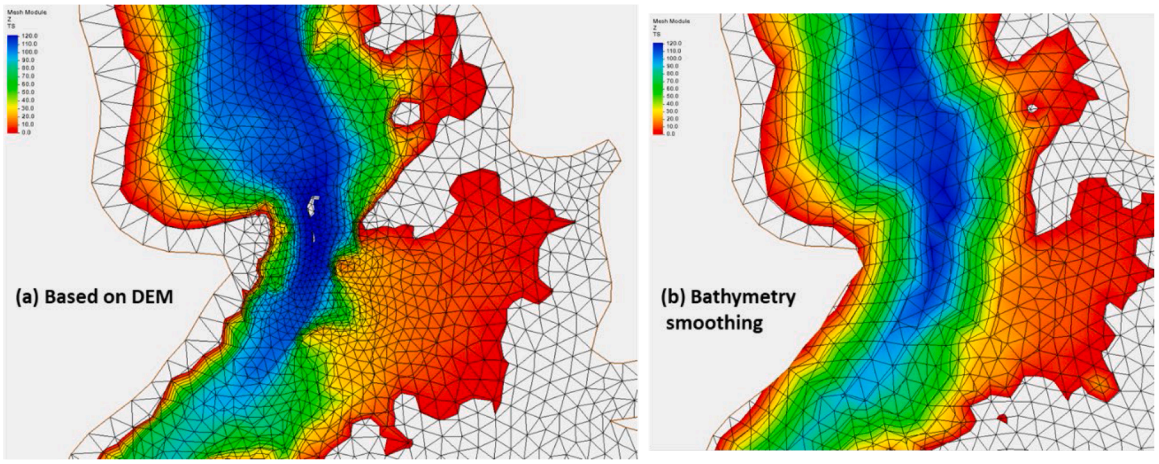

Fig. 8. Changes in bathymetry representation due to remeshing near the steepest slope (Thompson Point). (a) SCHISM mesh based on DEM; (b) Model A mesh showing a much-reduced slope due to heavy bathymetry smoothing/manipulation. Also note the coarser resolution in (b) near the slope; the smoothing/manipulation is however the main reason for the reduced slope.

4.1. Inter-connected mesh and DEM issues

In SCHISM, the mesh primarily serves as a vehicle to accurately represent the underlying topo-bathy features as revealed by the DEM. The first iteration of the mesh generation process has been illustrated in Section 3, which serves as a good starting point. However, mesh revisions are often necessary, due to calibration needs or DEM updates. In general, any DEM errors and uncertainties will directly affect SCHISM mesh and thus the model results; consequently, any updates in DEMs would generally require remeshing (e.g., re-alignment of the channel lines etc.) instead of simply interpolating the new DEM onto the old mesh (or a more egregious approach that uses the computational mesh as DEM and re-cycles the old mesh depths onto the new mesh). While expedient, the latter approaches defeat the purpose of the improved DEM quality. For this reason, we discuss the mesh and DEM issues together as this is an iterative process.

4.1.1. Lake Champlain

> Myth #1: Bathymetry smoothing/manipulation is harmless. Response: the results here and previously (Ye et al., Cai et al.) clearly indicated system altering biases will result from bathymetry smoothing/manipulation.

Despite its deficiency nearshore, the DEM used for this system is deemed to be of sufficient quality for the central basin and is thus used to revise the Model A mesh there, which has various problems as discussed below. Large discrepancies were observed of the bathymetry representation by the old and new mesh, as shown in Figs. 7, and 8. Note that except near Thompson Point (cf. Section 4.4.1), the two meshes have similar resolution and total mesh size; the main difference is how they represent the bathymetry. Besides the bathymetry smoothing that is evident in both regions, Model A mesh also contains many ad hoc fixes (cf. the jagged patterns in Fig. 7) beyond normal smoothing procedure, likely from the nearest-point interpolation method (NPI) used (more on this in Section 4.2).

To assess the sensitivity of SCHISM's skill with respect to meshes/

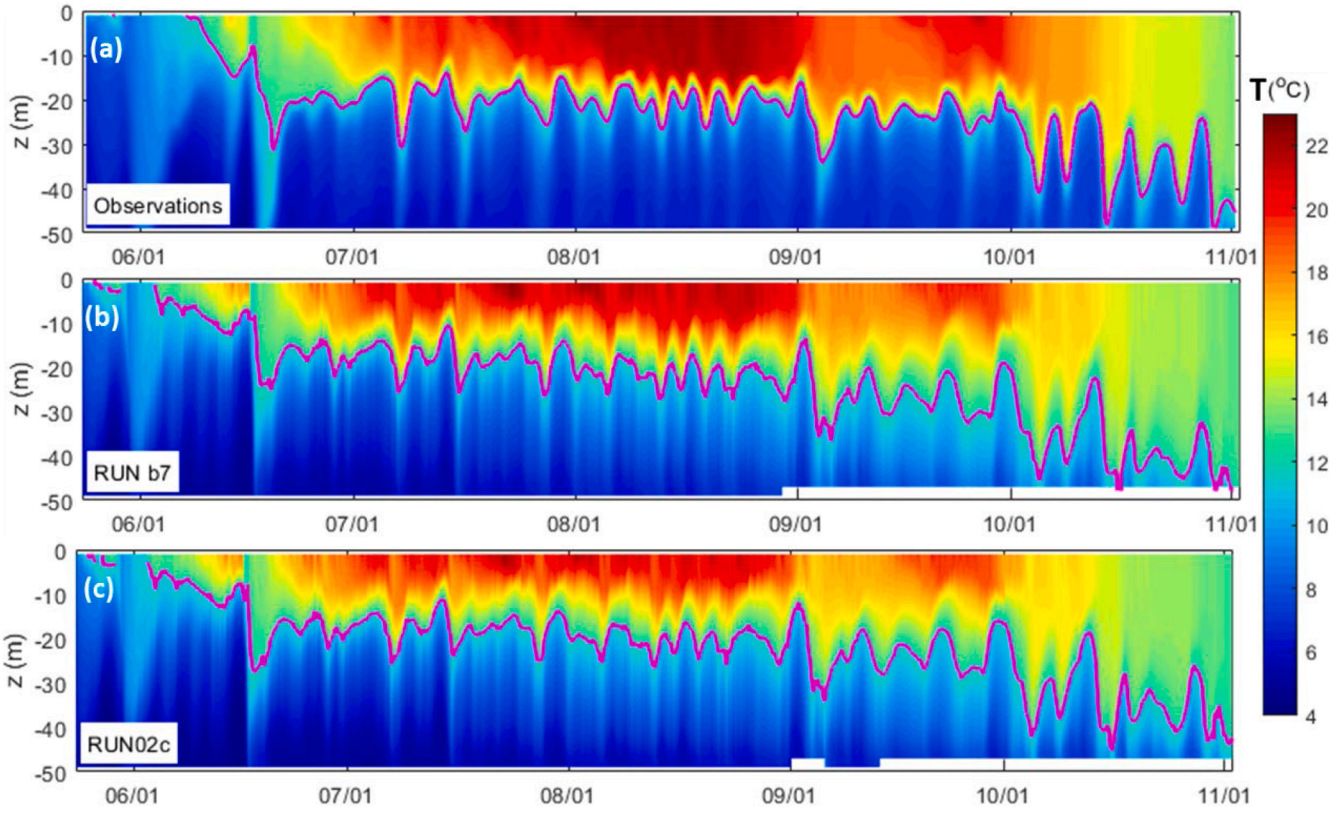

Fig. 9. Comparison of temperature profile at Valcour from *SCHISM* using two meshes. (a) Observation; (b) Model A mesh (32,685 nodes); (c) New mesh based on DEM (33,316 nodes). The pink lines are 12 °C isotherm. Only minor improvement is found at this station between (b) and (c).

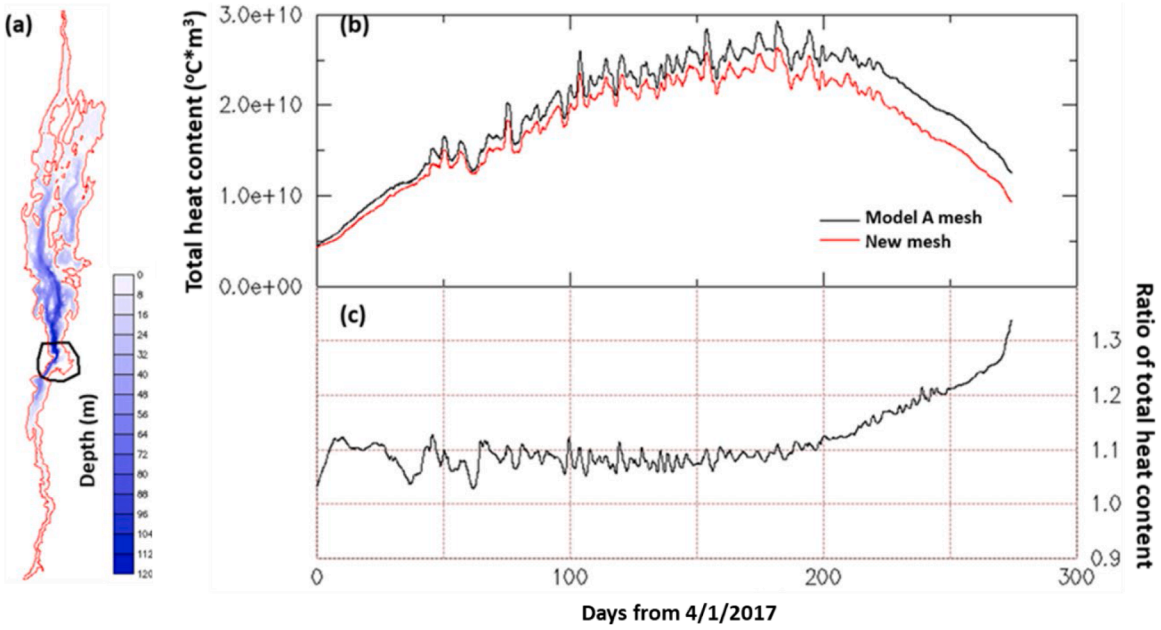

Fig. 10. (a) Bathymetry as seen by the new mesh, with the region with steeper bathymetric slope indicated, where remeshing was conducted using DEM. The region was used in the calculation of total heat content. (b) Comparison of total heat calculated by SCHISM in the region using Model A mesh and new mesh; (c) Ratio of total heat (Model A mesh)/(new mesh).

bathymetry, we compared the temperature profiles at Valcour island (Fig. 9). The comparison in Fig. 9 would suggest that the mesh redesign based on DEM has only resulted in minor differences, when a same model (SCHISM) is used. This cannot be further from the truth if one examines the system response. Different treatments of DEM and meshes have led to large differences in the total heat content in the area with steeper slopes (Fig. 10). This is because the smoothed bathymetry has led to a more mixed temperature profile over time in that region and warmer temperature in the hypolimnion, which accounts for most of the water column (as the thermocline is located ~15 m depth). The warmer temperature results in a larger heat content (Fig. 10b). While the bias in the total heat content is somewhat obscured by the high temperature above the thermocline (epilimnion) in the summer, the error increases from spring-summer (~10 %) to fall substantially (20–30 %) as fall

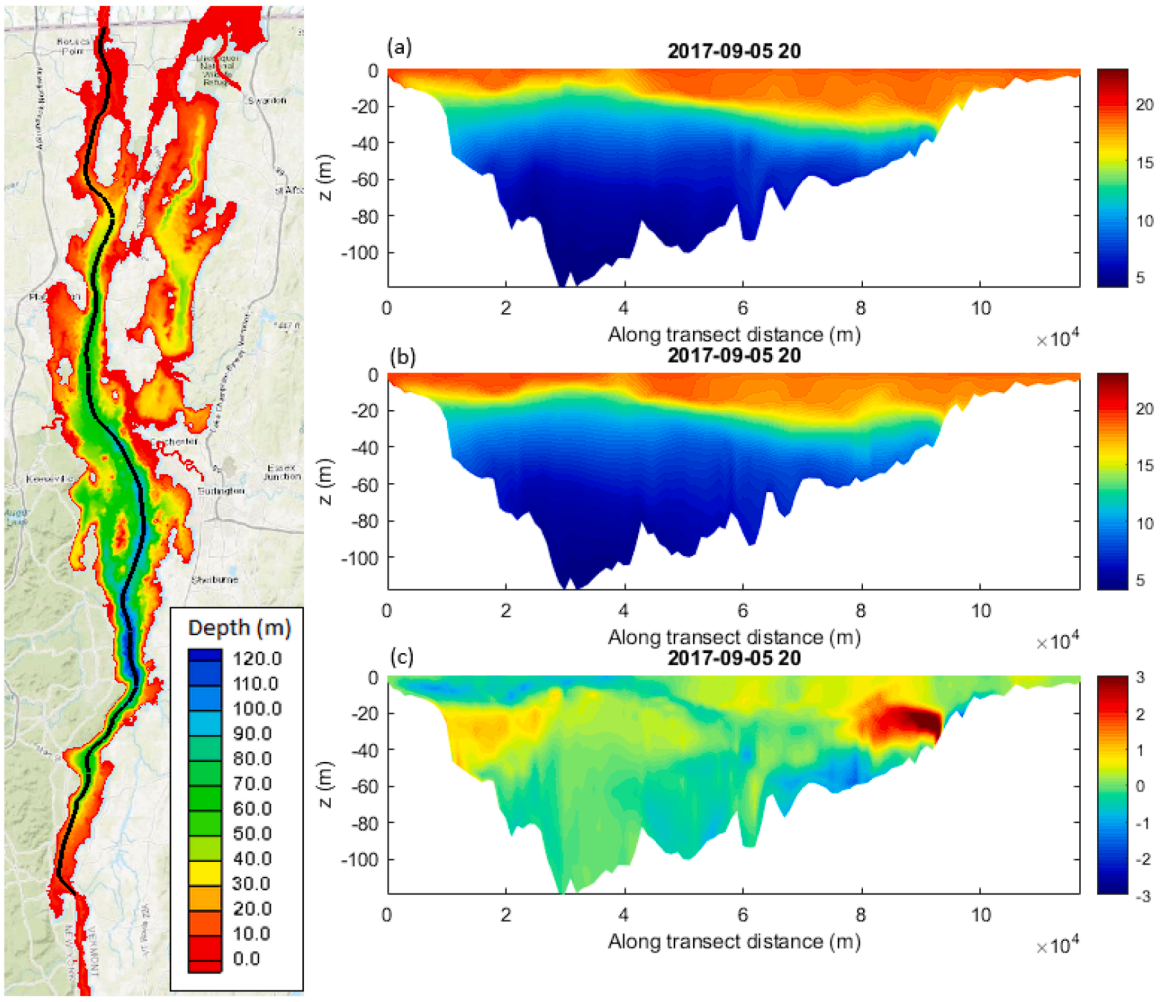

Fig. 11. Comparison of SCHISM's temperature profiles along the transect from south to north (shown on the left panel) between (a) new mesh based on DEM; (b) Model A mesh; (c) difference (a) - (b).

overturning occurs, because the warmer bottom water is mixed upward under the old mesh. This example illustrates the importance of process-based assessment (the 3rd principle) that looks at the system level response and the danger of assessing a model solely based on point-wise station comparisons; the effect of smoothing has indeed induced a system-wide change. Another piece of evidence of this system-wide change is shown in Fig. 11 along a south-north transect. The snapshot coincides with a strong southerly wind which results in downwelling in the north (right side of the figure). At some locations, the results are warmer and some locations cooler. In the north ($x = 90$ km), the new mesh leads to significantly deeper downwelling. In the south, the new mesh shows more upwelling of cooler waters near the surface.

4.1.2. *New York harbor*

An extreme case (but common among many models) of bathymetry manipulation is shown in Fig. 12, from Model A for NYH. Besides the obvious shortcoming of not resolving the channels [especially important for 3D processes; Fig. 12(b) and (d)], the mesh exhibits many ad hoc fixes, presumably to stabilize the model or improve skill (Fig. 12). The manipulation includes both the usual bathymetry smoothing that widens the channel (by making the channel depths shallower and shoal depths deeper, in order to preserve the volume; Fig. 12(ab)) but also some unexplained alterations, presumably adopted to enhance the model skill. For example, Fig. 12c indicates that the entire Harlem River part of the mesh should be dry or very shallow based on DEM. The bathymetry as seen in the Model A mesh (Fig. 12d), on the other hand, shows a much widened and artificially 'dredged' channel (also note that the model uses only 1 row of elements across the channel there). Even the most aggressive NPI with the channel greedy method (cf. Section

Myth #2: since DEMs have errors/uncertainties, modelers can freely manipulate them to improve the model.
Response: Manipulating DEMs leads to systemic changes that are often hard to compensate. The defensible approach is to work with the data provider to rectify the DEM errors and redo the mesh after that.
Success story: rectifying DEM errors by working with data provider is one of the best ways to improve model, as it removes a major error source and avoids error compensation.

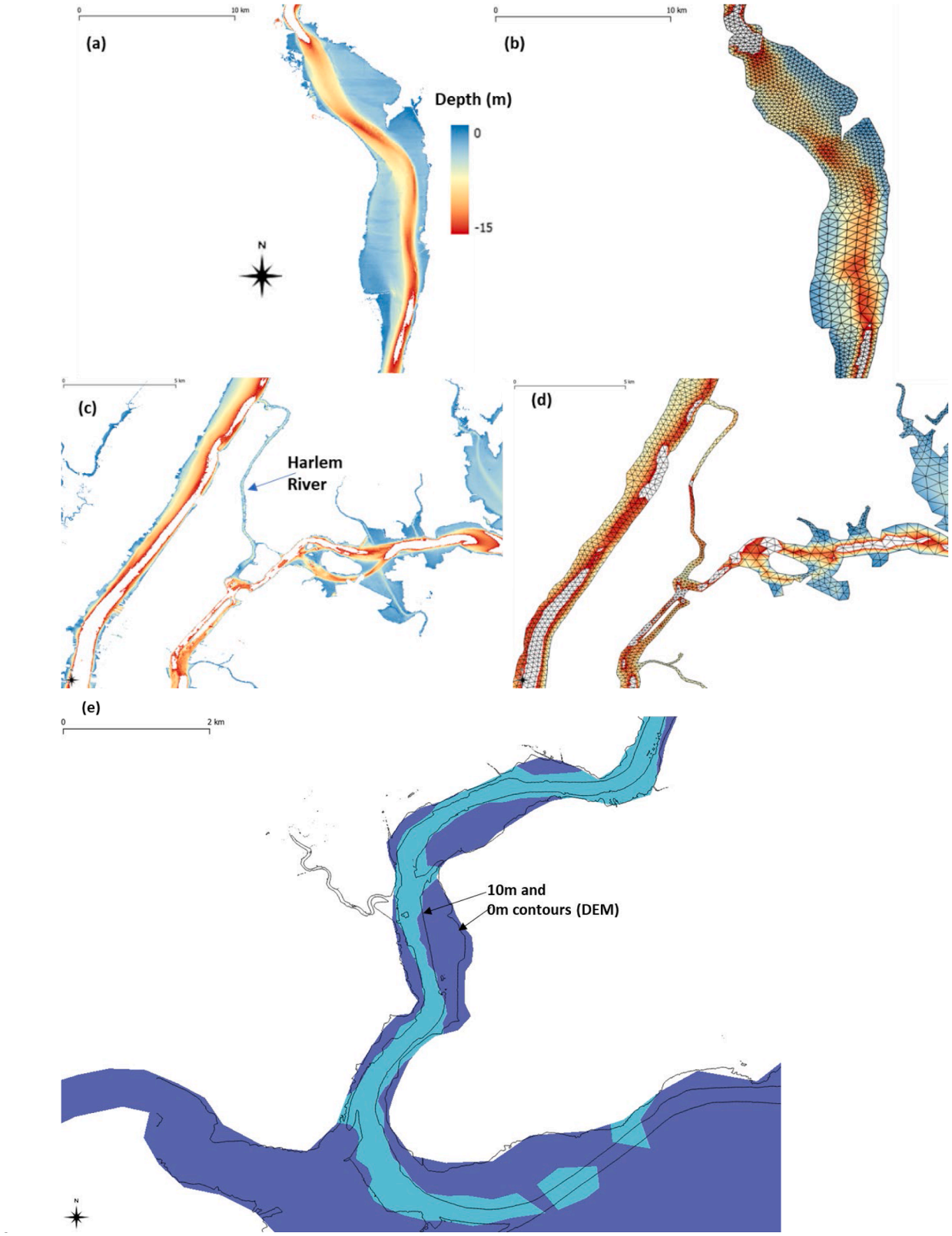

Fig. 12. Issues with Model A mesh for NYH case. (a,b) DEM and model mesh in Hudson River respectively. The blank areas inside the channels indicate depth greater than 15 m; (c,d) DEM and mesh near Harlem River respectively. (e) Overlay of bathymetry contours in Arthur Kill: the lines are from DEM, and the colors from the mesh (the light blue-green area is at least 10 m deep, and the blue area is at least 0 m deep).

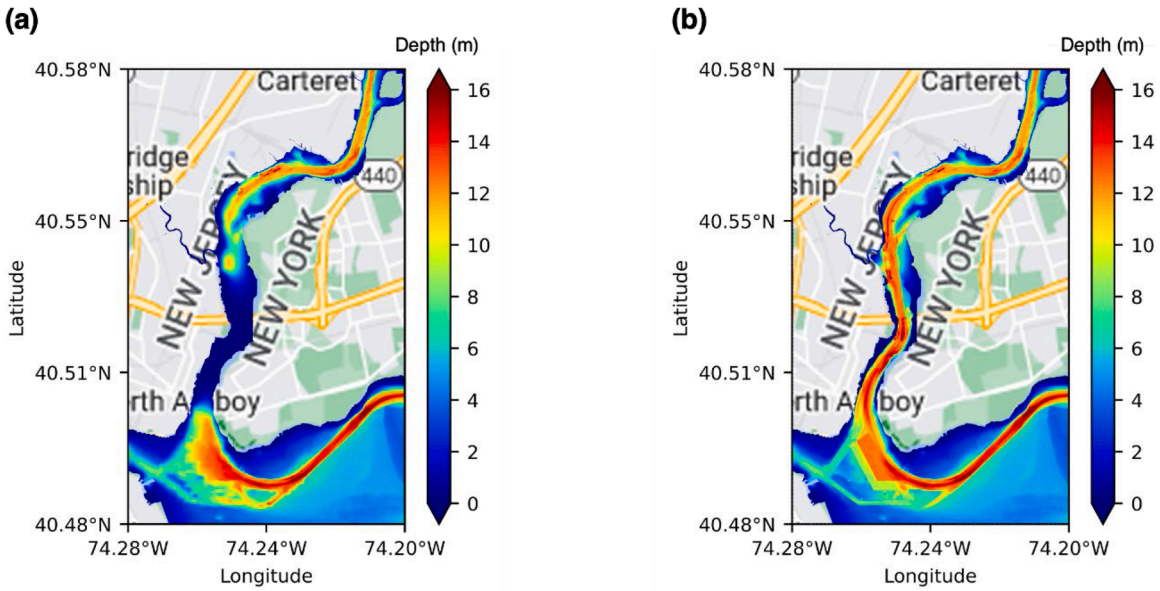

Fig. 13. (a) DEM issue near Arthur Kill showing a partially blocked channel in the old DEM; (b) New DEM from NOAA.

4.2) cannot explain the resultant depths as seen in Fig. 12d. Fig. 12e shows a quantitative comparison of depth contours in Arthur Kill; the model channel is usually wider than the actual channel by up to 100 % and misrepresents the natural variation of channel width in multiple places. In addition, the shoal depths are also substantially over-estimated through artificial dredging. These manipulations are several orders of magnitude larger than the DEM uncertainties (TVU). As demonstrated in the previous case, these errors will certainly induce system-level errors.

Next, we show that improving DEM quality is a sure way to improve SCHISM skill, because the model has been demonstrated to be able to realistically capture processes. The DEM used in the UFS project was composed from different topographic and bathymetric surveys (Table 2). During the early phase of the UFS project, the DEM included an erroneous survey that was discovered in the Arthur Kill channel (from Raritan Bay to Newark Bay) and resulted in effectively blocking part of the channel (Fig. 13a). The NOAA team was able to quickly identify the error and correct it using other bathymetry sources. The revised DEM shows a continuous navigation channel there (Fig. 13b). Remeshing was then carried out to accurately reflect the channel position as shown in the new DEM, and as a result, tides were able to propagate into the channel and Newark Bay (Fig. 14), as consistent with the harmonics observation. For example, the M2 tidal amplitude at Port Reading is improved from ~0.2 m to 0.75 m (vs. observed 0.76 m).

We stress here that DEM and mesh are closely connected to each other in the sense that, as shown here, revision in DEM should normally trigger remeshing in order to faithfully capture the updated features in the DEM. Probably due to the burden of mesh generation, we notice a common (mal)practice in the UG community that tends to bypass the remeshing step and simply re-interpolate the new DEM onto the old mesh. Expedient as this may be, it blunts a key advantage of UG modeling in capturing localized processes. Therefore, it is crucial that users maintain an efficient and *reproducible* workflow from beginning (DEM & meshing) to end (analysis such as time series extraction).

4.2. *Bathymetric interpolation*

> Myth #3: all interpolation methods are equally valid in modeling.
> Response: this is true only in the convergence sense, i.e., if the mesh resolution is close to DEM's resolution, which is often not the case. With typical resolution used, discontinuous methods like NPI can lead to large biases.

We use NYH case here to illustrate the systematic differences resulted from using linear interpolation versus NPI, the latter being a non-continuous method. The NPI method is widely used in many models and is often accompanied by a 'channel greedy' fix, i.e., the deepest depth in the nine raster cells of the DEM around a mesh point of interest is taken as the mesh depth. A well-known peculiarity of NPI is its discontinuous behavior as the mesh point is slightly nudged. While in theory all consistent interpolation methods will converge to the true DEM as the mesh is refined, the mesh size used in most models is far from fine enough to avoid the biases shown below. Historically, the channel-greedy fix was sometimes used to compensate for the shallow-biased harbor surveys, but this should be no longer necessary with the modern high-resolution survey data.

We compare SCHISM results obtained using the different interpolation methods. Using NPI for the NYH case, the total volume in the Arthur Kill channel is increased by a moderate 8.5 %. A station comparison for the surface and bottom salinity reveals some differences (Fig. 15b). However, the system response is much greater, as shown in Fig. 15(c) and (d); both seaward volume and tracer transports in the channel are decreased by over 40 % using the NPI approach. Like bathymetry smoothing, the results here demonstrate that interpolation methods used can significantly influence the model performance at the system level.

4.3. Post-processing and remeshing

Myth #4: modelers can relocate stations to improve the model.
Response: in silico oceanography calls for rigorous validation using the exact station location, as long as the DEM and station location are both accurate. This can avoid some surprises from localized processes.

An often-overlooked aspect of modeling occurs in the post-processing when users try to extract time series at a station. SCHISM uses linear interpolation method to extract station time series, which is consistent with the linear shape function used in the finite-element method. Most observation stations are located near the shoreline and sometimes sheltered by jetties due to ease of maintenance. Therefore, with insufficient mesh resolution deployed near the stations, an often-encountered issue is wetting and drying 'contaminating' the model results. An example is shown in Fig. 16 from the NYH case. The initial model results showed truncated tides at low water due to this issue (Fig. 16c). We remark that this artifact would be absent if a nearest-wet-node interpolation (a very popular method) were used. As described in Huang et al. (2022), rigorous validation can be achieved by using linear interpolation and making sure that the shoreline near the station is well resolved (Fig. 16). This illustrates the importance of the 2nd principle (adequate resolution on a needed basis).

4.4. Evidence based calibration

Myth #5: mesh generation involves many ad hoc decisions.
Response: while it is true that mesh generation involves many decision points that seem arbitrary among different users, keeping the central role of DEM in mind would minimize the differences. Often process-based assessment can be readily accomplished with minimal effort. Ideally, revision of the mesh should be evidence based, and in all cases, needs to be clearly justified.

Acknowledging the central role played by the DEM in modeling makes the calibration process significantly simpler because it removes a large source of error compensation. This is especially true if we focus on assessment of processes (the 3rd principle). The confounding error compensation among meshing and post-processing errors, DEM and forcing errors, and inherent model errors often makes the quantitative assessment challenging. Reducing the DEM, meshing and post-processing errors simplifies the process.

In this sub-section we describe the remaining calibration process associated with SCHISM, which mostly involves tuning parameters and mesh resolution/extent based on evidence from the model-data comparison. Admittedly, the quantitative assessment sometimes requires 'clever' compensation between inherent model errors and forcings errors. Due to the advancement in observation techniques, the forcings (and DEM) errors have been significantly reduced over the past two decades and the results presented in this paper give us hope that identifying model errors will become more transparent in the future, which will in return motivate model developers to focus on improving models.

4.4.1. Lake Champlain

Near steep slopes (as found near Thompson Point), the horizontal and vertical length scales become comparable, and therefore the hydrostatic assumption (horizontal >> vertical length scales) is at risk of being violated during meshing. Meshing near very steep slopes therefore requires some special care to avoid exacerbating this violation and is often an iterative process. We remark that this issue is usually encountered at steep slopes across shallow to deep depths (>100 m) in the baroclinic 'eddying regime' (Zhang et al., 2016). Fig. 17 shows two approaches we attempted. The SMS map shown in Fig. 17b over-refines near the steep slope such that the horizontal resolution near those narrow gaps is ~50 m, which is comparable to the vertical depth of ~50 m there, resulting in spurious upwelling, an exaggerated vertical velocity, and large vertical mixing (Fig. 17c). This can be understood from the finite-volume solver of the continuity equation used in SCHISM: the vertical velocity is inversely proportional to the horizontal element area and as a result, any errors in the calculated horizontal divergence directly translate to the vertical velocity as the mesh is refined. Fig. 17a relaxes the resolution locally so that the finest horizontal resolution is ~80 m. With adequate dissipation provided by a slope-dependent Shapiro filter, the model is able to suppress the spurious upwelling and maintain a sharp stratification at Thompson Point (Fig. 17d). Although different momentum dissipation could have been used with the mesh in Fig. 17b to obtain similar stratification as in Fig. 17d (not shown), tuning of dissipation amount would take some effort. Alternatively, if a fine resolution comparable to depth has to be used, a simple solution would be to reduce the time step (and in this case, other parts of the mesh may need to be refined as well because SCHISM requires CFL number not be smaller than 0.4) (Zhang and Baptista, 2008; Zhang et al., 2016).

4.4.2. New York harbor

Our experience with this case strongly suggests that following the 3 principles makes the model calibration process easier, because it minimizes the error compensation that would otherwise significantly confound the calibration process. Here we demonstrate two cases of model improvement based on evidence and hints from the model outputs and comparison with observation. We remark that this improvement would be impossible had we not resolved key system features based on DEMs.

Particularly challenging for models are those up estuary stations near the salt intrusion limit where the channels are substantially narrower. During the first phase of the UFS project, a persistent issue was identified

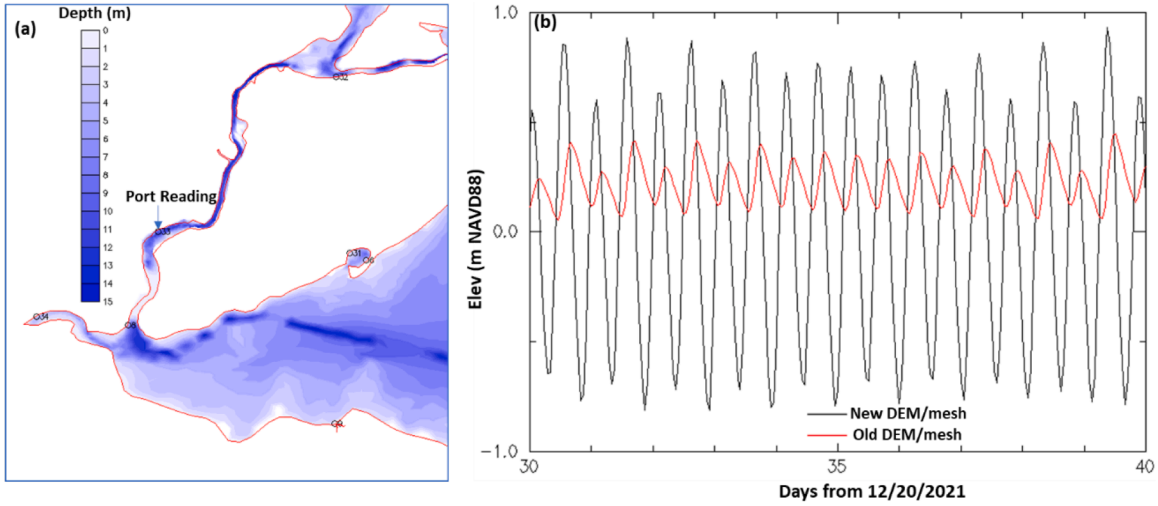

Fig. 14. Improvement of elevation at a gauge (Port Reading) in Arthur Kill. (a) Gauge location on top of bathymetry from old DEM, as seen by the old mesh, showing a partially blocked channel; (b) Comparison of elevation at Port Reading (from the 2D model with atmospheric and river forcing).

for the tidal elevation at an upper Hudson station (Piermont) where the model consistently under-estimated the amplitude. After ruling out DEM errors, we hypothesized that this under-estimation was due to the tidal reflection at the upstream river boundary. Extending the boundary farther upstream (Fig. 18a) indeed greatly reduced the error: the M2 amplitude at this station was increased from 0.41 m to 0.49 m (compared to 0.55 m from the observation). Incidentally, SCHISM was also able to obtain good results at this station with Model A mesh, but for the wrong reason: the water volume is greatly exaggerated in that mesh due to various manipulations (cf. Section 4.1.2). System-level checks

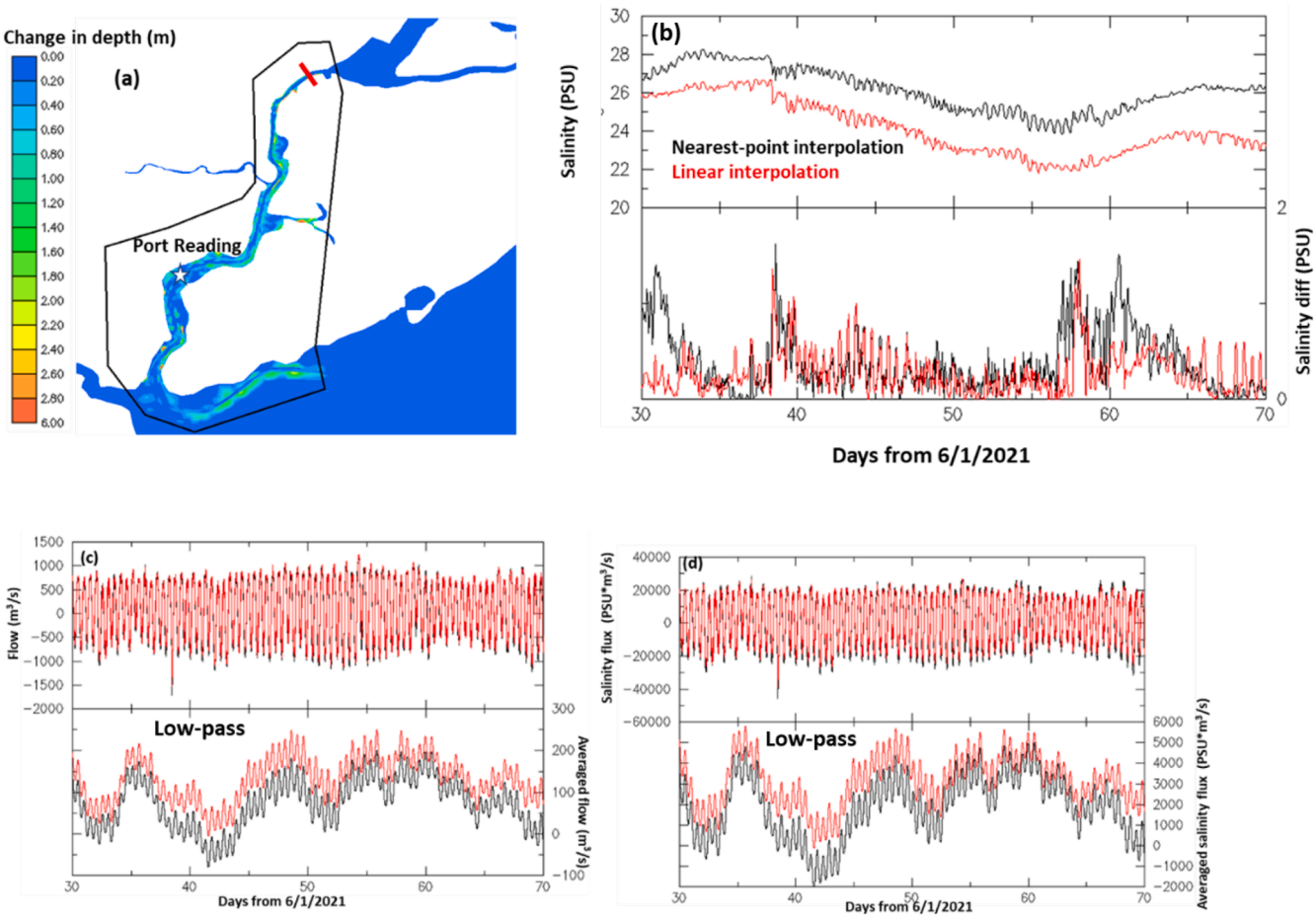

Fig. 15. Comparison of results using different bathymetric interpolation methods. (a) Region in which NPI is carried out. (b) Surface salinity and surface-bottom difference comparisons at gauge Port Reading (see (a) for location). (c) Volumetric transport at a transect (shown in (a) as a red line) and its 4-day running average (positive southward or out of estuary). The average flow from Day 30 to 70 indicates a difference of 44 %. (c) Salt flux and its 4-day running average at the transect; the average difference is 41 %. The fluxes are a better measure for system response.

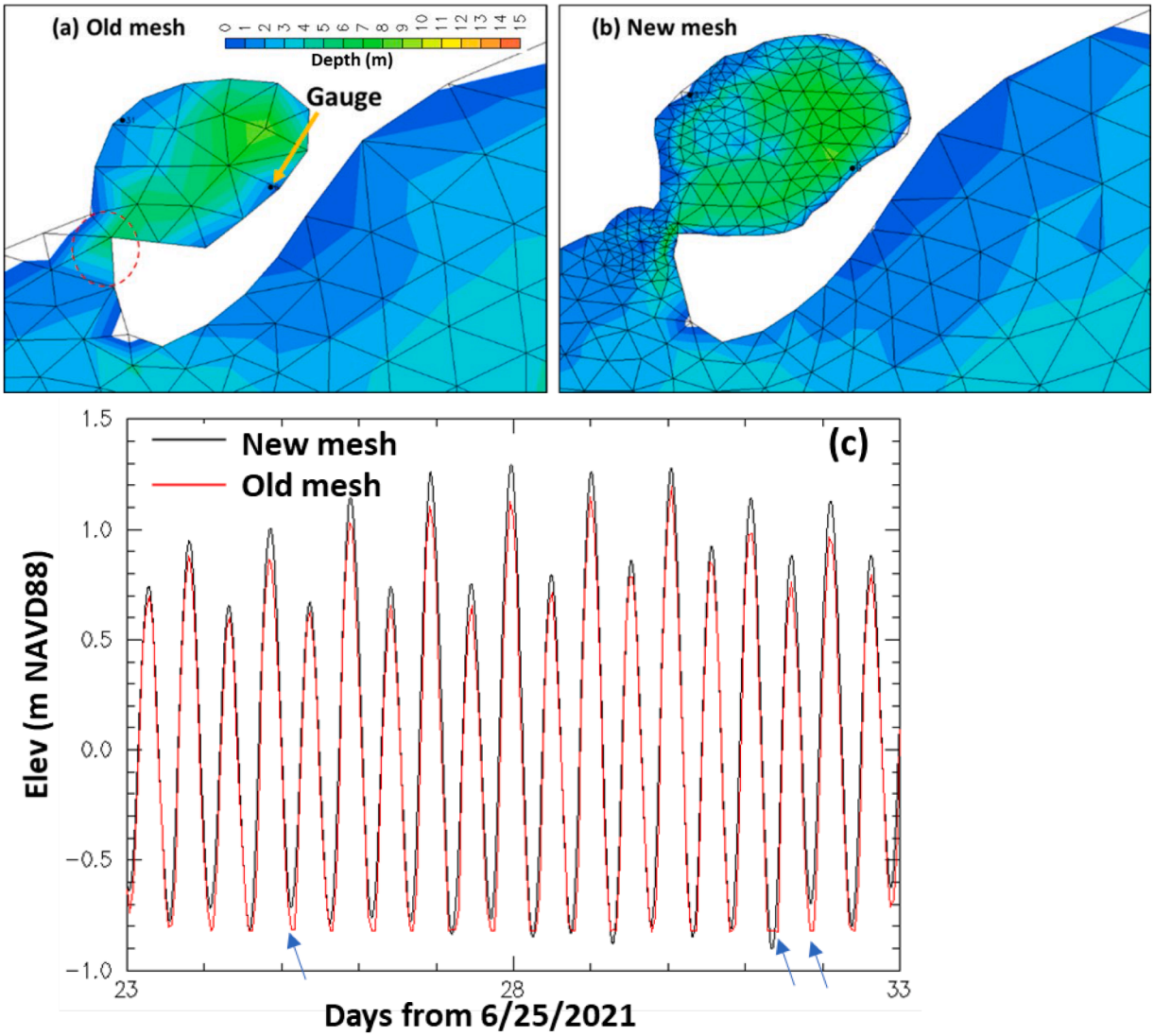

Fig. 16. An example of remeshing near wet/dry interface in the Great Kills Harbor to accurately capture the station elevation. (a) and (b) show the comparison of old and new (refined) mesh with gauge location. (c) Elevation comparison between old and new meshes showing the drying instances during ebbs in the old mesh (indicated by arrows). The red dashed circle in (a) shows the clogged harbor entrance.

like those in Section 4.1.1 can be used to reveal key differences in process representation such as salt fluxes, etc.

Another issue we encountered during the calibration phase was related to over-estimation of salinity at Harlem River (Fig. 19). The error source could come from several factors: local DEM, river flow, bottom friction value used, etc. Results from various sensitivity tests (not shown) eventually implicated the connection between Hudson and Harlem, and the mesh was subsequently refined locally near the confluence to ensure unimpeded exchange between the two (Fig. 19a). This brought down the salinity and made it closer to observation, although over-estimation at flood tide persisted. Minor local adjustment of diffusivity and friction can be used to further improve the model (not shown).

4.5. Numerical dissipation

Klingbeil et al. (2014) presented a theoretical framework that can be used to estimate the relative contributions of physical and numerical (spurious) dissipations to the total dissipation in finite-volume models, using the Discrete Variance Decay of the tracer as a metric. The tool is very useful to identify hot spots of mixing and can thus help model developers assess the origin of numerical dissipation in their models. However, it is clear from the current paper that the tool can be misused when comparing numerical dissipations across models, as different models often 'see' different fundamental forcings (such as bathymetry). An example was shown in Ye et al. (2018; Fig. 20) for the Chesapeake Bay channel: physical mixing occurs in non-smoothed bathymetry, e.g., near sharp corners that are often smoothed out by many models as part of the bathymetry smoothing procedure. This often leads to an erroneous conclusion that the models using smoothed bathymetry have low numerical dissipation. The unphysically low-mixing zone in the shoal can be clearly seen in Fig. 20c. This interplay among physical and numerical dissipations and forcings is not accounted for in Klingbeil's theoretical framework. Quantifying the errors in the forcing functions used in different models should be a top priority for future research.

4.6. Summary: qualitative vs. quantitative assessment

In our experience, the answer to process-based assessment (3rd principle) is often more straightforward and clear-cut than the

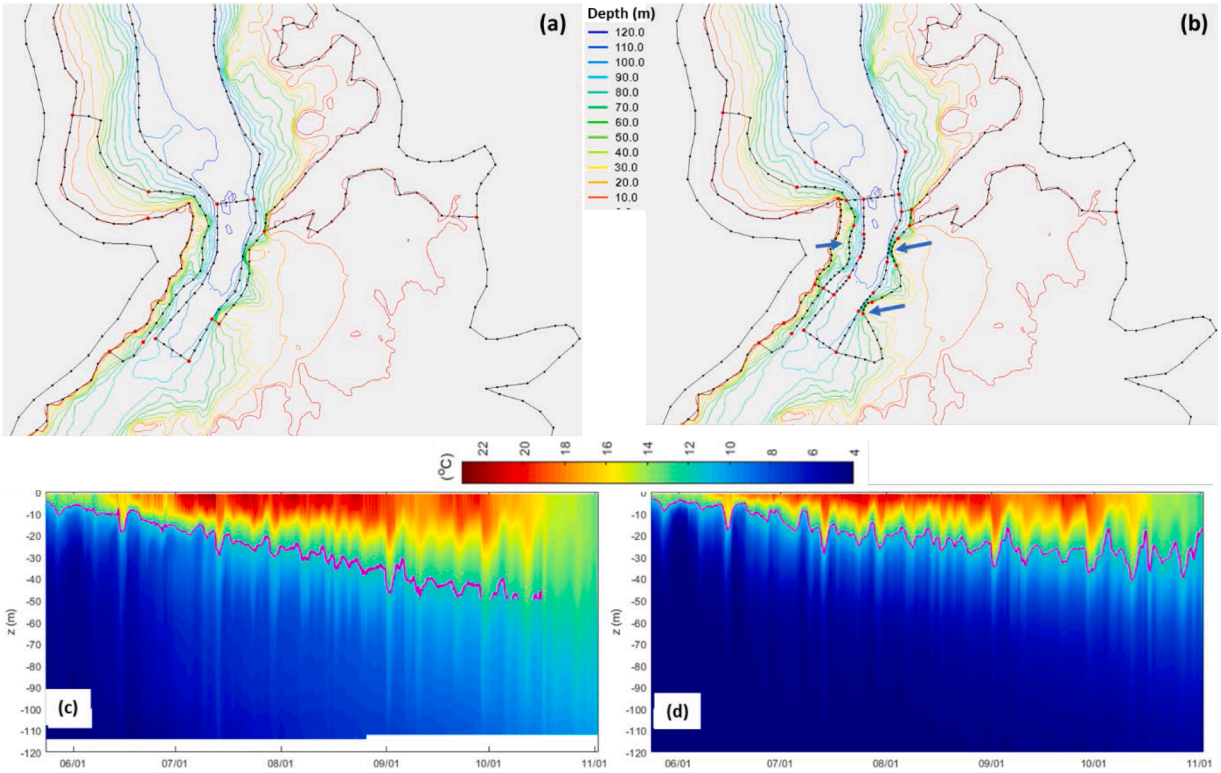

Fig. 17. (a,b) Two different meshing approaches near Thompson Point. The arrows point to places of over refinement in (b). (c,d) Resultant temperature profiles at Thompson Point from (b,a) respectively.

quantitative error metrics. Furthermore, focusing on processes makes the calibration process in SCHISM much simpler; it is often sufficient to conform mesh to DEM plus some simple calibration procedure based on evidence, as we have demonstrated in this section. In fact, results for the examples shown in Sections 4.1 to 4.3 were all obtained with a few iterations, an indication that our model, grounded on 'real' DEMs, is physically and numerically defensible in representing processes. Quantitative assessment, on the other hand, often requires extensive, time-consuming tuning that maximizes 'clever' error compensation and thus significantly muddies the bigger picture. As modern models become increasingly complex, there are potentially many tunable 'handles', e.g., it is a common practice to use different parameterization or mixing schemes to compensate for the errors in the atmospheric forcing.

The results from Sections 4.1 to 4.4 clearly demonstrate the central role played by DEM in defensible modeling. Acknowledging this helps to debunk many commonly held myths that coastal modeling lacks rigor; in fact, we believe that defensible modeling is already within reach by following the three principles described here. Short of this, relying on error compensation, particularly that involves tweaking DEMs/bathymetry to accommodate model needs, would result in system-wide biases that may go undetected by point comparisons. This practice is unfortunately prevalent in literature. We therefore strongly advocate a reassessment of many aspects of *in silico* oceanography with a different perspective that first focuses on process-based assessment before diving

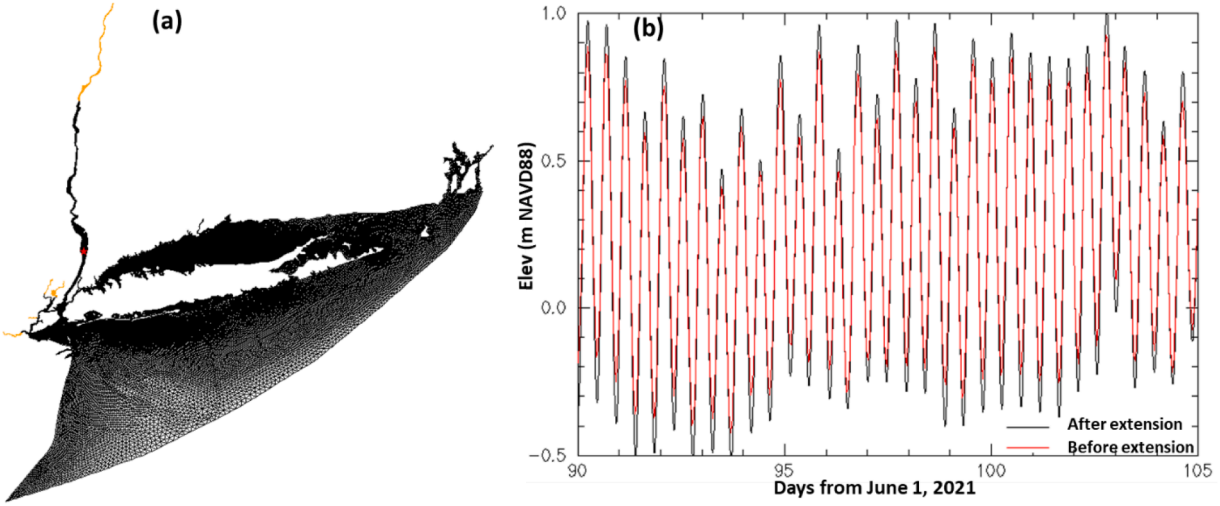

Fig. 18. Tidal reflection. (a) Extension of mesh for upstream Hudson River. (b) Improvement in tides at Piermont (the red star in (a); also see Fig. 5c for details).

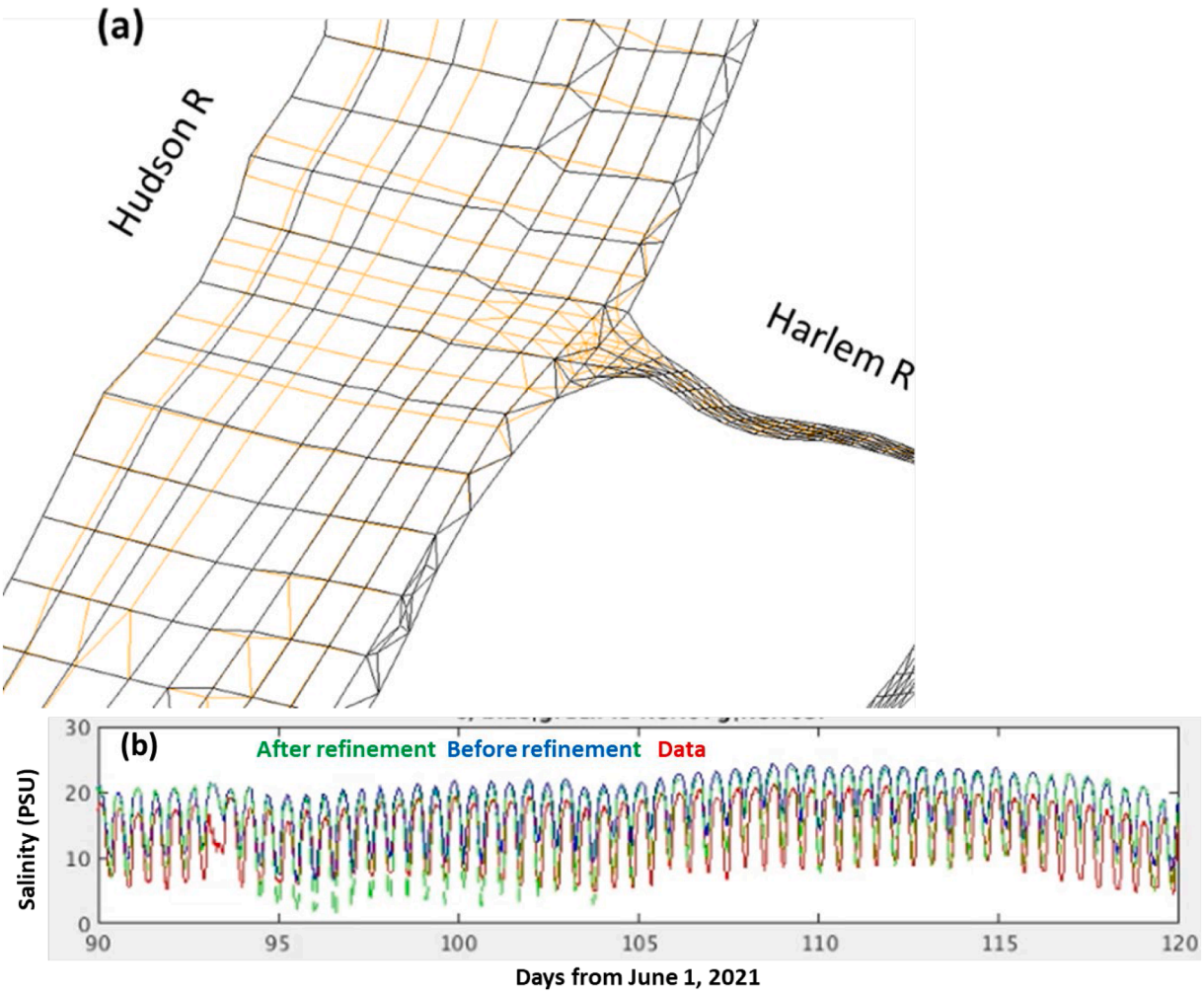

Fig. 19. (a) Grid refinement near the confluence of Hudson and Harlem Rivers to better capture the exchanges there (black is old mesh and orange is new mesh); (b) improvement in the surface salinity at a Harlem station (at Mill Pond).

into quantitative skill assessment. For the latter, evidence-based calibration is preferred. At the very least, modelers should fully disclose, preferably in a dedicated section, any alterations to DEM done in their study with well-reasoned justification. This philosophy is summarized as 'steering wheel of modeling', where DEM is front and center and must be honored in *all* aspects of modeling process, from mesh generation to preprocessing to model physics/numerics to model assessment and analysis (Fig. 21). This philosophy represents a paradigm shift from how coastal modeling was done.

While addressing the DEM issue is the first step toward defensible modeling, there are other types of important forcing functions such as boundary conditions, bottom friction, atmospheric forcing, etc. Quantifying these functions for numerical models may require advancement beyond modeling alone. We anticipate that observation techniques for these functions will continue to advance, which will push forward rigorous *in silico* oceanography in the next decade.

5. Conclusions

We demonstrated in this paper an important, gray, and often misunderstood area that plagues contemporary coastal modeling and makes it non-rigorous, i.e., how Digital Elevation Model (DEM) is treated in the models. We proposed three guiding principles: (1) bathymetry is a first order forcing in coastal domains and thus should be respected in all aspects of modeling; (2) oceanographic processes are driven across multiple spatial scales and so a model should enable appropriate resolution as needed; (3) assessment should focus on processes.

Using a community model (SCHISM) and two realistic test cases involving a freshwater lake and a typical estuarine system, we demonstrated that defensible modeling is already within reach by following the three principles. Detailed guidelines were proposed for unstructured mesh generation that are centered on honoring the underlying DEM. In fact, DEM must be adhered to in the entire modeling process from mesh generation to model physics/numerics to the post analysis. We also showed that focusing on process-based assessment makes the calibration process much simpler.

In the next two decades, we anticipate that rapid improvement in observation techniques in coastal oceanography will further reduce the uncertainties in DEM and other forcing functions needed in *in silico*

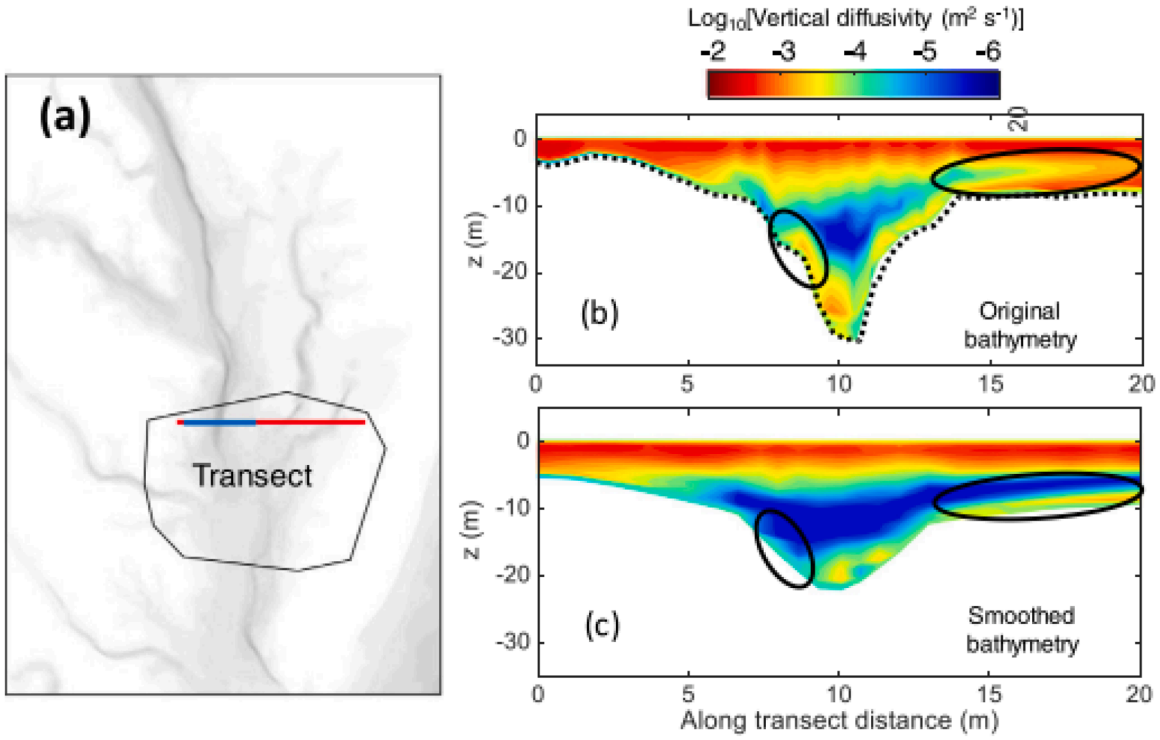

Fig. 20. Effects of bathymetry smoothing on vertical mixing as illustrated for Chesapeake Bay. (a) The region (enclosed by the polygon with black lines) where bathymetry smoothing is done and the transect (red and blue lines) used in analysis; (b) time averaged vertical diffusivity along the blue portion of the transect with the original bathymetry; (c) same as (b) but with the smoothed bathymetry. The dashed line in (b) shows the bottom profile from the original high-resolution DEM. The ellipses in (b) and (c) highlight the locations (steep slope and shoal) of the most obvious changes in mixing patterns. Plots are time averaged from May to October in 2012. Reproduced from Fig. 14 of Ye et al. (2018) with permission by Elsevier. [This article was originally published in Ocean Modelling, Vol. 127, page 16–39, by Ye, F., Zhang, Y., Wang, H., Friedrichs, M.A.M., Irby, I.D., Alteljevich, E., Valle-Levinson, A., Wang, Z., Huang, H., Shen, J., Du, J. as "A 3D unstructured-grid model for Chesapeake Bay: importance of bathymetry", Copyright Elsevier (2018)].

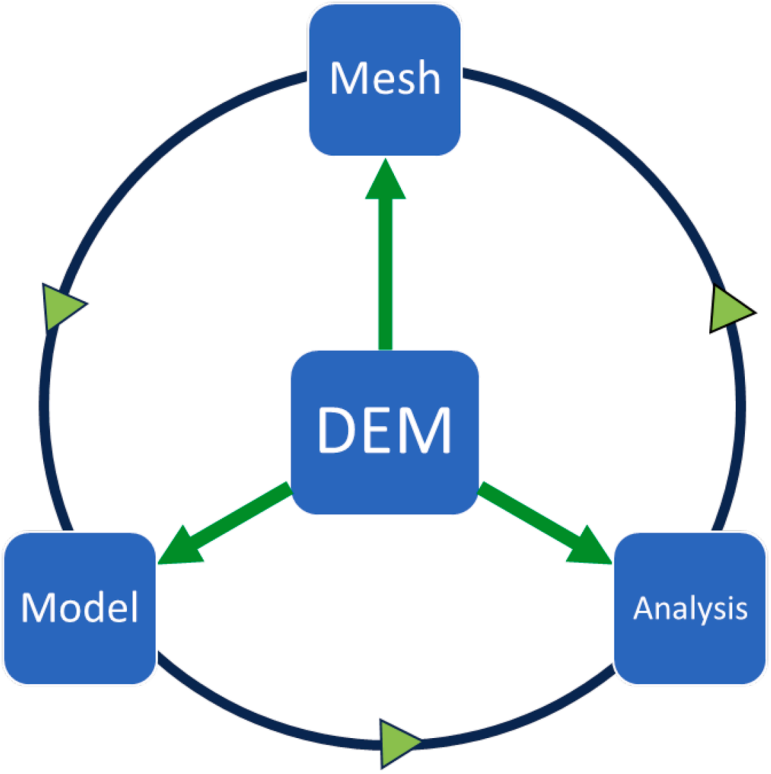

Fig. 21. Steering wheel of coastal modeling.

oceanography, thus further enhancing the scientific rigor. However, future models cannot take full advantage of this advancement unless they make a paradigm shift away from manipulating bathymetry/DEM.

Supplementary Materials

Model related files for the two cases presented in this paper can be downloaded at Zenodo (https://doi.org/10.5281/zenodo.10656035). The SCHISM version used is v5.10.0.

CRediT authorship contribution statement

Y. Joseph Zhang: Methodology, Formal analysis, Validation, Writing – original draft, Writing – review & editing. **Joshua Anderson:** Writing – original draft, Visualization, Validation, Investigation, Formal analysis, Data curation. **Kyungmin Park:** Visualization, Validation, Methodology, Investigation, Formal analysis, Data curation. **Chin H. Wu:** Funding acquisition, Supervision, Project administration, Validation, Writing – original draft, Writing – review & editing. **Spenser Wipperfurth:** Validation, Investigation. **Eric Anderson:** Writing – original draft, Writing – review & editing. **Shachak Pe'eri:** Project administration, Writing – original draft, Writing – review & editing. **Dmitry Beletsky:** Funding acquisition, Supervision, Writing – original draft, Writing – review & editing. **Daniel Titze:** Project administration, Writing – original draft, Writing – review & editing. **Emanuele Di Lorenzo:** Funding acquisition, Supervision, Writing – original draft. **Saeed Moghimi:** Writing – original draft, Project administration, Writing – review & editing. **Gregory Seroka:** Writing – review & editing, Writing – original draft, Project administration. **Edward Myers:** Writing – original draft, Project administration. **Ayumi Fujisaki-Manome:** Writing – original draft, Writing – review & editing. **John Kelley:** Writing – original draft, Methodology, Writing – review & editing.

Declaration of competing interest

The authors declare that they have no known competing financial interests or personal relationships that could have appeared to influence the work reported in this paper.

Data availability

Data shared via Supplemental Materials.

Acknowledgements

This study was funded by NOAA grants: #NA22NOS4730223, #NA23NOS0120063 and #NA17OAR4320152; the last grant provided partial funding for this work through the International Joint Commission Lake Champlain-Richelieu River Study; the funding was awarded to the Cooperative Institute for Great Lakes Research (CIGLR) through the NOAA Cooperative Agreement with the University of Michigan. . The authors thank Dr. Antonio Baptista for fruitful discussions on the principles of *in silico* oceanography. Simulations used in this paper were conducted using the following computational facilities: (1) William & Mary Research Computing (URL: https://www.wm.edu/it/rc); (2) Texas Advanced Computing Center (TACC), The University of Texas at Austin. This is CIGLR Contribution No. 1243 and NOAA GLERL Contribution No. 2053.

References

Anderson, J.D., Zhang, Y., Titze, D., Beletsky, D., Cannon, D., Feyen, J., Wu, C.H., 2024. The spatial and temporal structure of internal waves in Lake Champlain, to be submitted to Ocean Modelling.

Beletsky, D., Titze, D., Kessler, J., Mason, L., Fry, L., Read, L., Saunders, W., Chu, P.Y., Feyen, J., Lee, D., Kelly, J.G.W., 2022. NOAA Technical Memorandum GLERL-179. https://doi.org/10.25923/2hy2-ca15.

Benjamin, S.G., Weygandt, S.S., Brown, J.M., Hu, M., Alexander, C.R., Smirnova, T.G., Olson, J.B., James, E.P., Dowell, D.C., Grell, G.A., Lin, H., 2016. A North American hourly assimilation and model forecast cycle: the rapid refresh. Mon. Weather Rev. 144 (4), 1669–1694.

Cai, X., Zhang, Y., Shen, J., Wang, H.V., Wang, Z., Qin, Q., Ye, F, 2020. A numerical study of hypoxia in chesapeake bay using an unstructured grid model: validation and sensitivity to bathymetry representation. J. Am. Water Resour. Assoc. 1–24. https://doi.org/10.1111/1752-1688.12887.

ECCC (2015) Development of an experimental 2D hydrodynamic model of Lake Champlain using existing bathymetric data (Task 1-2) Report.

Fringer, O.B., Dawson, C.N., He, R., Ralston, D.K., Zhang, Y., 2019. The future of coastal and estuarine modeling: findings from a workshop. Ocean Model 143, 101485.

Holleman, R., Fringer, O., Stacey, M., 2013. Numerical diffusion for flow-aligned unstructured grids with application to estuarine modeling. Int. J. Numer. Meth. Fluids 72, 1117–1145. https://doi.org/10.1002/fld.3774.

Hood, R.R., Shenk, G.W., Dixon, R.L., Smith, S., Ball, W.P., Bash, J.O., Batiuk, R., Boomer, K., Brady, D.C., Cerco, C., Claggett, P., de Mutsert, K., Easton, Z.M., Elmore, A.J., Friedrichs, M., Harris, L.A., Ihde, T.F., Lacher, L., Li, L., Linker, L.C., Miller, A., Moriarty, J., Noe, G.B., Onyullo, G.E., Rose, K., Skalak, K., Tian, R., Veith, T.L., Wainger, L., Weller, D., Zhang, Y., 2021. Chesapeake bay program modeling system: overview and recommendations for future development. Ecol. Modell. 456, 109635.

Huang, W., Zhang, Y., Wang, Z., Ye, F., Moghimi, S., Myers, E., Yu, H., 2022. Tidal simulation revisited. Ocean Dyn. 72, 187–205. https://doi.org/10.1007/s10236-022-01498-9.

IHO (2020) International hydrographic organization standards for hydrographic surveys, S-44, https://iho.int/uploads/user/pubs/standards/s-44/S-44_Edition_6.1.0.pdf.

Klingbeil, K., Mohammadi-Aragh, M., Gräwe, U., Burchard, H., 2014. Quantification of spurious dissipation and mixing - discrete variance decay in a finite-volume framework. Ocean Modell. 81, 49–64.

Klingbeil, K., Lemarié, F., Debreu, L., Burchard, H., 2018. The numerics of hydrostatic structured-grid coastal ocean models: state of the art and future perspectives. Ocean Modell. 125, 80–105. https://doi.org/10.1016/j.ocemod.2018.01.007. Pages.

Park et al. (2024) Evaluation of a 3D Unstructured Grid Model under Different Forcing Sources, Ocean Modelling, to be submitted to VSI: in silico oceanography via seamless cross-scale modeling: are we there yet?

Pe'eri, S., Parrish, C., Azuike, C., Alexander, L., Armstrong, A., 2014. Satellite remote sensing as a reconnaissance tool for assessing nautical chart adequacy and completeness. Marine Geod. 37 (3), 293–314. https://doi.org/10.1080/01490419.2014.902880.

Skopeliti, A., Stamou, L., Tsoulos, L., Pe'eri, S., 2020. Generalization of soundings across scales: from DTM to harbour and approach nautical charts. ISPRS Int. J. Geo.-Inf. 9, 693. https://doi.org/10.3390/ijgi9110693.

Titze, D., Beletsky, D., Feyen, J., Saunders, W., Mason, L., Kessler, J., Chu, P., Lee, D., 2023. Ocean Dyn. 73, 231–248. https://doi.org/10.1007/s10236-023-01550-2.

Umlauf, L., Burchard, H., 2003. A generic length-scale equation for geophysical turbulence models. J. Mar. Res. 6, 235–265.

Wilkin, J., Rosenfeld, L., Allen, A., Baltes, R., Baptista, A., He, R., Hogan, P., Kurapov, A., Mehra, A., Quintrell, J., Schwab, D., Signell, R., Smith, J., 2017. Advancing coastal ocean modelling, analysis, and prediction for the US integrated ocean observing system. J. Oper. Oceanogr. 10, 115–126.

Ye, F., Zhang, Y., Wang, H., Friedrichs, M.A.M., Irby, I.D., Alteljevich, E., Valle-Levinson, A., Wang, Z., Huang, H., Shen, J., Du, J., 2018. A 3D unstructured-grid model for Chesapeake Bay: Importance of bathymetry. Ocean Modell. 127, 16–39.

Ye, F., Zhang, Y., He, R., Wang, Z., Wang, H.V., Du, J., 2019. Third-order WENO transport scheme for simulating the baroclinic eddying ocean on an unstructured grid. Ocean Modell. 143, 101466 https://doi.org/10.1016/j.ocemod.2019.101466.

Ye, F., Cui, L., Zhang, Y., Wang, Z., Moghimi, S., Myers, E., Seroka, G., Zundel, A., Mani, S., Kelley, J.G.W., 2023. A parallel Python-based tool for meshing watershed rivers at continental scale. Environ. Modell. Softw. 166, 105731 free access for 50 days. https://authors.elsevier.com/c/1hAc-4sKhEZH1K.

Zhang, Y., Baptista, A.M., Myers, E.P., 2004. A cross-scale model for 3D baroclinic circulation in estuary–plume–shelf systems: I. Formulation and skill assessment. Cont. Shelf Res. 24, 2187–2214.

Zhang, Y., Baptista, A.M., 2008. SELFE: a semi-implicit Eulerian–Lagrangian finite-element model for cross-scale ocean circulation. Ocean Modell. 21 (3–4), 71–96.

Zhang, Y., Ateljevich, E., Yu, H.-C., Wu, C.-H., Yu, J.C.S., 2015. A new vertical coordinate system for a 3D unstructured-grid model. Ocean Modell. 85, 16–31.

Zhang, Y., Ye, F., Stanev, E.V., Grashorn, S., 2016. Seamless cross-scale modeling with SCHISM. Ocean Modell. 102, 64–81. https://doi.org/10.1016/j.ocemod.2016.05.002.